

**POLITECNICO DI MILANO**  
**Facoltà di Ingegneria Industriale**  
**Corso di Laurea in Ingegneria Aerospaziale**



**Preliminary design of an on-board  
de-orbiting system for Block I**

**Relatore: Prof. Luigi DeLuca**

**Correlatore: Prof. Valery I. Trushlyakov**

**Progetto di:**

**Marco Fassina 721152**

**21 dicembre 2010**

**Anno accademico 2009/2010**



## ABSTRACT

In order to prevent a huge amount of space debris around earth orbit space agencies look for new solution to mitigate, reduce or avoid the problem. The solution proposed in this work, developed from the initial bases posed at Omsk Technical State University, consider the possibility to use the unused propellant left in tanks as a source of energy. The gasification of this unused propellant should give the necessary thrust to complete a maneuver of de-orbiting to bring the stage in a disposal orbit or down to earth. In particular it has been developed a system for the gasification of the Block I, the third stage of Soyuz. In order to design this system it has been developed a model to simulate the process of evaporation of the liquid.

Al fine di prevenire una smisurata crescita della spazzatura spaziale presente nell'orbita terrestre, le agenzie spaziali stanno cercando diverse soluzioni per affrontare il problema. La soluzione proposta in questo lavoro di tesi, le cui basi sono state poste presso la Omsk Technical State University, considera la possibilità di utilizzare il propellente non utilizzato presente nei serbatoi come risorsa di energia. Gasificando questo propellente residuo si deve generare una spinta tale da permettere il completamento della manovra di de-orbiting che consente di portare il sistema o in un'orbita di parcheggio oppure farlo precipitare verso la Terra. In particolare è stato sviluppato un sistema attivo di de-orbiting per il Block I, ossia il terzo stadio della Soyuz. Per poter dimensionare il sistema di gasificazione è stato sviluppato un modello con lo scopo di simulare il processo di evaporazione del propellente non utilizzato.



## CONTENTS

---

1	Introduction	3
1.1	Motivations	3
1.2	Tasks	4
1.3	Presentation plan	4
2	State of the art	7
2.1	Historical evolution of the russian launcher Soyuz	7
2.2	Technical features	8
2.2.1	The first stage - Strap on Booster	10
2.2.2	The second stage - Core stage	11
2.2.3	The third stage - Block I	11
2.2.4	The upper stage - Fregat	14
2.2.5	Soyuz: a general review	16
2.3	Problem of the space debris	21
2.3.1	Categories of space debris	22
2.3.2	Debris generation: some examples	24
2.3.3	Space debris: sources	26
2.4	Generalities about de-orbiting systems	27
2.4.1	Definition of passivation	27
3	Mission analysis	29
3.1	Mission profile	29
3.1.1	Phase 1	29
3.1.2	Phase 2	33
3.1.3	Phase 3	33
3.2	De-orbiting mission profile	34
4	Description of the problem	37
4.1	Description of the problem	37
4.2	Description of components	38
4.2.1	RP-1	38
4.2.2	Liquid oxygen	46
4.2.3	In-flow mixture choice	47
5	Analytic Model	59
5.1	Convection-based Model	59
5.2	Diffusion-based Model	64
5.3	Results	64
6	Preliminary design of the system	79
6.1	System design	79
7	Conclusions	83
7.1	future development	83



## LIST OF FIGURES

---

Figure 1	The Soyuz stages	9
Figure 2	Strap on booster	10
Figure 3	Core stage	12
Figure 4	The Block I	13
Figure 5	The Fregat	15
Figure 6	The Soyuz-U	17
Figure 7	The Soyuz-FG	18
Figure 8	The Soyuz-2	19
Figure 9	The Soyuz-ST	20
Figure 10	Space debris dispersion	22
Figure 11	Debris evolution after object explosion	25
Figure 12	Typical mission profile	29
Figure 13	Velocity profile	30
Figure 14	Acceleration profile	31
Figure 15	Dinamic pressure profile	31
Figure 16	Pitch angle profile	32
Figure 17	Altitude versus distance profile	32
Figure 18	Altitude versus time profile	33
Figure 19	Upper stage typical profile	34
Figure 20	$\Delta v$ versus $\alpha$	36
Figure 21	Dodecane molecular structure	42
Figure 22	Propane molecular structure	42
Figure 23	Isopentane molecular structure	43
Figure 24	Isohexane molecular structure	44
Figure 25	n-Hexane molecular structure	44
Figure 26	Benzene molecular structure	45
Figure 27	Methylcyclopentane molecular structure	45
Figure 28	n-Heptane molecular structure	45
Figure 29	1,3-dimethylcyclopentane molecular structure	46
Figure 30	Methylcyclohexane molecular structure	46
Figure 31	Toluene molecular structure	46
Figure 32	Mass flow into the tank for RP <sub>1</sub> -LOX at O/F = 2.34	50
Figure 33	Mass flow into the tank for RP <sub>1</sub> -LOX at O/F = 3.3	52
Figure 34	Mass flow into the tank for UDMH-NTO at O/F = 2	53
Figure 35	Mass flow into the tank for UDMH-NTO at O/F = 2.9	54
Figure 36	Mass flow into the oxidizer tank for RP <sub>1</sub> -LOX at O/F = 2.34	55

Figure 37	Mass flow into the oxidizer tank for RP1-LOX at O/F = 3.3	56
Figure 38	Mass flow into the oxidizer tank for UDMH-NTO at O/F = 2	57
Figure 39	Mass flow into the oxidizer tank for UDMH-NTO at O/F = 2.9	58
Figure 40	$h$ versus acceleration ratio	63
Figure 41	$T_{gas}$ versus $T_{in}$ fuel tank	65
Figure 42	$T_{gas}$ versus $h$ fuel tank	65
Figure 43	$T_{gas}$ versus $\dot{m}_{in}$ fuel tank	66
Figure 44	$T_{liq}$ versus $T_{in}$ fuel tank	66
Figure 45	$T_{liq}$ versus $h$ fuel tank	67
Figure 46	$T_{liq}$ versus $\dot{m}_{in}$ fuel tank	67
Figure 47	$T_{gas}$ versus $T_{in}$ fuel tank diffusive model	68
Figure 48	$T_{gas}$ versus $h$ fuel tank diffusive model	68
Figure 49	$T_{gas}$ versus $\dot{m}_{in}$ fuel tank diffusive model	69
Figure 50	$T_{liq}$ versus $T_{in}$ fuel tank diffusive model	69
Figure 51	$T_{liq}$ versus $h$ fuel tank diffusive model	70
Figure 52	$T_{liq}$ versus $\dot{m}_{in}$ fuel tank diffusive model	70
Figure 53	$T_{gas}$ versus $T_{in}$ oxidizer tank	71
Figure 54	$T_{gas}$ versus $h$ oxidizer tank	72
Figure 55	$T_{gas}$ versus $\dot{m}_{in}$ oxidizer tank	72
Figure 56	$T_{liq}$ versus $T_{in}$ oxidizer tank	73
Figure 57	$T_{liq}$ versus $h$ oxidizer tank	73
Figure 58	$T_{liq}$ versus $\dot{m}_{in}$ oxidizer tank	74
Figure 59	$T_{gas}$ versus $T_{in}$ oxidizer tank diffusive model	74
Figure 60	$T_{gas}$ versus $h$ oxidizer tank diffusive model	75
Figure 61	$T_{gas}$ versus $\dot{m}_{in}$ oxidizer tank diffusive model	75
Figure 62	$T_{liq}$ versus $T_{in}$ oxidizer tank diffusive model	76
Figure 63	$T_{liq}$ versus $h$ oxidizer tank diffusive model	76
Figure 64	$T_{liq}$ versus $\dot{m}_{in}$ oxidizer tank diffusive model	77
Figure 65	presentation of different kind of injector	82
Figure 66	Performances of injector	82
Figure 67	$M_{liq}$ trend for LOX and RP-1	83
Figure 68	comparison of $M_{liq}$ trend for RP-1	84
Figure 69	comparison of $M_{liq}$ trend for LOX	84



## LIST OF TABLES

---

Table 1	Souyz family evolution	9
Table 2	First stage features	11
Table 3	Second stage features	12
Table 4	Third stage features	14
Table 5	The upper stage features	16
Table 6	Main featuers of Soyuz-U	17
Table 7	Main featuers of Soyuz-FG	18
Table 8	Specifications of Soyuz-2 launch vehicle	19
Table 9	Power capability of Soyuz-2 launch vehicle	19
Table 10	Power capacity of Soyuz-ST launch vehicle	20
Table 11	Specifications of Soyuz-2-3 launch vehicle	21
Table 12	Soyuz-2-3 launch vehicle power capacity	21
Table 13	Composition of tracked space debris	22
Table 14	Estimated amount of debris by size	24
Table 15	Percntage incidence of explosions causes	26
Table 16	RP-1 and compounds properties [1]	42
Table 17	RP-1 evaporation components [2]	43
Table 18	Theoretical Performance of Liquid Rocket Propellant Combinations	48
Table 19	Mass flow composition into tank for RP <sub>1</sub> -LOX at O/F = 2.34	49
Table 20	Mass flow composition into tank for RP <sub>1</sub> -LOX at O/F = 3.3	51
Table 21	Mass flow composition into tank for UDMH-NTO at O/F = 2	51
Table 22	Mass flow composition into tank for UDMH-NTO at O/F = 2.9	53
Table 23	Mass flow composition into oxidizer tank for RP <sub>1</sub> -LOX at O/F = 2.34	54
Table 24	Mass flow composition into oxidizer tank for RP <sub>1</sub> -LOX at O/F = 3.3	55
Table 25	Mass flow composition into oxidizer tank for UDMH-NTO at O/F = 2	56
Table 26	Mass flow composition into oxidizer tank for UDMH-NTO at O/F = 2.9	57
Table 27	Typical coefficient for heat transfer covvection [3]	59
Table 28	Aluminum properties	80
Table 29	Nozzle conditions	81
Table 30	Performance parameters	81

Table 31      Nozzle features      81

## INTRODUCTION

---

### 1.1 MOTIVATIONS

On 4 October 1957 Soviet Union launched the *Sputnik 1*, the first launch of a satellite made by mankind. Since that moment and for the next 50 years there is been a race to the conquest of the space. In the following years after the launch of *Sputnik 1*, in the middle of the cold war, have been put in orbit a lot of others space probes and satellites, especially by Russia and United States of America.

For the first 30 years of space colonization no one space agency cared about the increase level of man-made pollution, and no one thought that on the threshold of the twenty-first century pollution could become one of the most serious problem for the continuation of human spread in earth orbit. As a result of this great space activity, a huge amount of debris has been left orbiting around Earth.

An introductory definition of orbital debris could be the following: orbital debris is any human-made object in orbit that no longer serves a useful purpose. It could be discarded equipment, rocket stages, defunct satellites, bolts and other hardware released during deployment of satellites, and fragments from the breakup of satellites and rocket stages.

In the early 80's space pollution started to concern scientists and space agencies, so in this period have been posed the basis for a preliminary regulatory on orbital debris and its control. Even if there is been this first approach at the problem, significant efforts are seen only in the 90's due to an increased activity of *NASA*, and partnerships with *ESA*, particularly.

Nowadays every space agency and commercial company knows the problem of space debris and makes great efforts in its mitigation and control. Especially new technologies with the aim of producing less fragments for each launch, developed tracking capability and a series of general rules for preventing debris generation are working to make the near earth orbit safer for the next space expansion.

## 1.2 TASKS

The main goal of this work is to do a preliminary design of an on-board de-orbiting system for the third stage of the Russian launcher *Soyuz*, in particular it is been taken under consideration the **Block I**, that is the third stage of *Soyuz*. There are different way to develop an on-board de-orbiting system, the most used is "passivation", that briefly consist in the prevention of breakups by eliminating every kind of residual energy, as residual propellants in tanks, residual energy in batteries or left energy in pressure system, gyros and so on, contained in a stage or spacecraft at the end of its life.

The *Block I* is already equipped with a system for avoiding collision and de-orbiting, that consist in venting the liquid oxygen tank, in this work is going to define another kind of de-orbiting system that is based on a different philosophy. Seen that after the end of his mission in the tanks of the stage are left about the 3% of residual propellants unused, we want to exploit completly, or at least the more as possible this residual energy to make a manuever for a faster and safer reentry of the stage. Through the evaporation of this residual propellants we want to obtain a thrust that forced this stage in a faster reentry. Gasification is made by a system which introduce in tanks warm gases, with temperature in a range of 700K - 900K, that heat the the gas and liquid presents in the tanks and by heat exchange from gas and liquid we obtain the evaporation of residual propellants. Once reached a pressure of 5atm are opened the valves that conduct a mass flow to a nozzle, that expels these gases and produce the thrust necessary to the maneuver.

## 1.3 PRESENTATION PLAN

The presentation of this work is articulated in this way:

- **Chapter 2:** in this chapter is discussed the state of the art. It is reported general and technical features of the russian launcher *Soyuz* and its history. In the second part is discussed the problem of space debris in all its facets, as definition, hazard, methods for prevention and mitigation, and are also reported few examples of how debris could be generate. At the end is introduced the theme of de-orbiting system and "passivation", as one of the way to make the near earth space safer.
- **Chapter 3:** here is analyzed a typical mission profile made by *Soyuz* and the performances of the launcher. In the second part is analyzed the mission profile for de-orbiting the system and is evaluated the  $\Delta v$  necessary to complete this maneuver.

- **Chapter 4:** this part analyzes the properties of the propellant elements and contain the studies for the chemical characterization of the propellant budget for the active de-orbiting system
- **Chapter 5:** this chapter contains the analytic model used to reproduce the process of gasification of residual propellants in tanks. Through this model it is also possible to define the features useful to design the on-board de-orbiting system.
- **Chapter 6:** this chapter contains a very preliminary design for the system of gasification that should be equipped on Block I to obtain a thrust necessary to de-orbit the satge.
- **Chapter 7:** this chapter contain the conclusion of the work.



## STATE OF THE ART

---

### 2.1 HISTORICAL EVOLUTION OF THE RUSSIAN LAUNCHER SOYUZ

The **Soyuz** is the most recent of a long line of *Soyuz family* vehicles, that have had great success since their construction thanks to its low cost and high reliability. *Soyuz* launcher takes its origin from another russian launcher, the *Voskhod*, with the scope of putting in orbit the manned *Soyuz* spacecraft.

The three-stage version known as *Soyuz*, first introduced in 1966, has been launched more than 850 times. Due to their close technical similarity (same lower three stages), the *Molniya* and *Soyuz* vehicles are commonly combined together for reliability calculations. In the last 25 years they have completed a success rate of 98,1% over more than 950 launches. As the primary manned launch vehicle in Russia and the former Soviet Union, and as today one of the primary transport to the *International Space Station*, the *Soyuz* has benefited from these standards in both reliability and robustness. The addition of the flexible, restartable *Fregat* upper stage in 2000 allows the *Soyuz* launch vehicle to perform a full range of missions (LEO, SSO, MEO, GTO, GEO, and escape).

The *Soyuz* is launched from the Baikonur Cosmodrome in Kazakhstan, from the Plesetsk Cosmodrome in the North of Russia and from the Guiana Space Center in French Guiana to meet the needs of the commercial market and continuing to serve the needs of Russian government and other institutional and international programs. *Soyuz* launch vehicles continue to be mass-produced in Samara, Russia, by the Samara Space Center, whose facilities have been designed to accommodate the production of up to four launch vehicles per month. As a result of the continued demand from the Russian government, International Space Station activity, and commercial orders, the *Soyuz* launcher is in uninterrupted production at an average rate of 10 to 15 vehicles per year with a capability to rapidly scale up to accommodate users' needs.

The *Fregat* upper stage production by NPO Lavochkine, Moscow, Russia is well suited with this production rate.

Several improvements were made on the vehicle's design during the 1960ies and early 1970ies, cumulating in 1973 with the introduction of the *Soyuz U*, which unified and standardized the improvements that had been made over the previous eight years.

The *Soyuz U2* has been introduced in 1982 and used synthetic kerosene ("Sintin") in the core stage to provide higher performance.

In 1999, a restartable upper stage *Ikar* based on the Kometa satellite bus has been added to the lower three-stages of the *Soyuz U*. This configuration has allowed the Soyuz to reach circular orbits above 500km, and has been used for six flights to deploy half (24 satellites) of the Globalstar constellation.

In 2000 the Soyuz has begun to adopt the *Fregat* upper stage. It has a larger propellant capacity than the *Ikar* stage, and is also restartable.

In 2001 the first and second stages engine have been upgraded. This improvement primarily has involved modifying the injector pattern for the engines to improve the propellant mixing and combustion, hence raising the overall specific impulse.

Later even the third stage engine has been upgraded and changed with an improved variant [4].

In the table 1 it is possible to recognize the most important phases of development of russian launchers that have brought to the actual configuration of the *Soyuz*.

## 2.2 TECHNICAL FEATURES

As already said *Soyuz* is medium-lift launcher made by three stages plus an upper stage, that could be used to place satellites or to bring astronauts or cargo on the International Space Station. The main performances and characteristics of this vehicle are:

- **Payload:** 3,150kg delivered to geostationary transfer orbit (GTO), and up to 4,900kg into Sun-synchronous orbit (with a circular altitude of 820km);
- **Reliability:** it is the world's most launched vehicle, with over 1,700 manned and unmanned missions performed by the Soyuz family to date;
- **Versatility:** An exceptionally versatile launcher, perfectly suited for GTO mid-range payloads, medium-Earth orbit (MEO), low-Earth orbit (LEO) and Sun-synchronous satellites, as well as Earth escape missions.

In figure 1 is represented a view of the four stages of the launcher.

It is going to be exposed in particular the most important features of the stages which compose the launcher.



Period of activity	Model
1957 – 1960	RA-7/Sputnik 1 (no longer in production)
1958 – 1991	Vostok (no longer in production)
1960–	Molniya (Four-stage LV with block I as third stage)
1963 – 1976	Voskhod (Three-stage LV with block I as third stage) (no longer in production)
1966 – 1976	Soyuz (Voskhod upgrade to support Soyuz spacecraft) (no longer in production)
1973–	Soyuz U (Unified LV to replace Voskhod and Soyuz)
1982 – 1995	Soyuz U2 (Soyuz U upgrade for using of "Sintin") (no longer in production)
1999	Soyuz U (Introduction of Ikar upper stage)
2000	Soyuz U (Introduction of Fregat upper stage)
2001	soyuz U (Introduction of upgraded 1st and 2nd stage engines, RD-107A and RD-108A)
2004 – 2006	Soyuz U (Introduction of ST fairing and upgraded 3rd stage engine RD-124)

Table 1: Soyuz family evolution

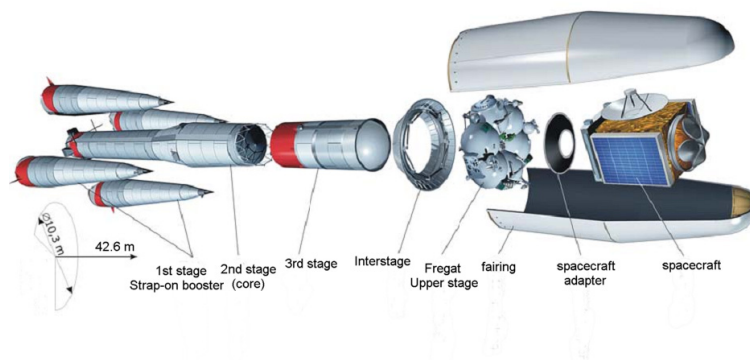


Figure 1: The Soyuz stages

### 2.2.1 The first stage - Strap on Booster

The four boosters (see fig. 2) are arranged around the central core and are tapered cylinders with the oxidizer tank in the tapered portion and the kerosene tank in the cylindrical portion. As in the entire Soyuz lower composite, the *RD-107A* engines of the boosters are powered by nontoxic liquid oxygen – kerosene propellants. These spark-ignition engines are fed by a turbopump running off gases generated by the catalytic decomposition of  $H_2O_2$  in a gas generator. Each *RD-107A* has four combustion chambers and nozzles. Liquid nitrogen is used for pressurization of the propellant tanks.

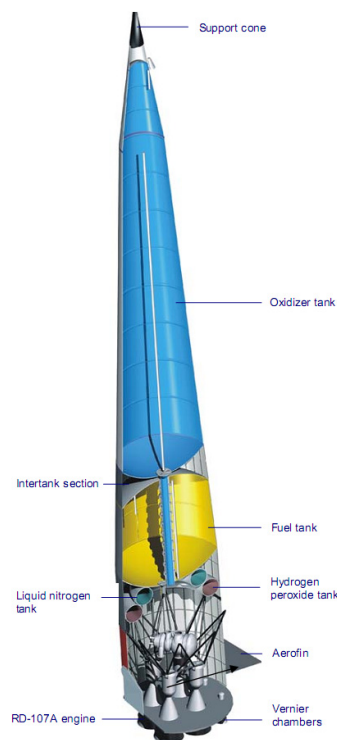


Figure 2: Strap on booster

Attitude control is carried out through two movable vernier thrusters and one aerofin. Three-axis flight control is made possible through these eight engines (two per booster) and four aerofins (one per booster).

The boosters burn for 118 seconds and are then discarded. Thrust is transferred through a ball joint located at the top of the cone-shaped structure of the booster, which is attached to the central core by two rear struts[4].

<b>Size</b>	2.68m diameter x 19.60m length
<b>Gross/Dry mass</b>	44,413kg / 3,784kg
<b>Propellant</b>	27,900kg LOX 11,260kg Kerosene
<b>Structure</b>	Pressure stabilized aluminium alloy tanks with intertanks skin structure
<b>Propulsion</b>	RD-107A 4-chambers engine
<b>Thrust</b>	838.5kN SL; 1021.3kN Vac
<b>Isp</b>	262s – SL; 319s –Vac
<b>Feed system</b>	pump-fed by hydrogen peroxide gas generator
<b>Pressurization</b>	Liquid nitrogen vaporization
<b>Burn time / Restart</b>	118s / No (two level thrust throttling)
<b>Attitude Control</b>	Two 35kN vernier thrusters and one aerofin
<b>Avionics</b>	Input/Output units, TM, power
<b>Stage separation:</b>	Pyronuts/pushers/reaction nozzle

Table 2: First stage features

### 2.2.2 The second stage - Core stage

The second stage (see fig. 3) is similar in construction to the booster stages, using the *RD-108A* engine and four vernier thrusters for three-axis flight control. The core stage nominally burns for 290 seconds. The stage is shaped to accommodate the boosters, and a stiffening ring is located at the upper interface between the boosters and central core. This structure is strengthened with use of larger fairing.

The boosters and the central core are ignited on the ground. They burn at intermediate thrust levels for approximately 20 seconds before actual liftoff in order to verify their health and nominal level of operation. The core stage continues to function after booster shutdown and separation[4].

### 2.2.3 The third stage - Block I

Ignition of the third stage' single main engine occurs approximately 2 seconds before shutdown of the central core. The separation of the stages takes place at a predetermined velocity. After separation, the lower skirt of the third stage is jettisoned in three sections.

The third stage of the Soyuz is powered by the *RD-0110* engine (see fig. 4). The LOX and kerosene tanks will be modified to accommodate the more powerful *RD-0124* engine. In fact, since the *RD-0110* and *RD-0124* engines have the same thrust, the same stage structure can accommodate

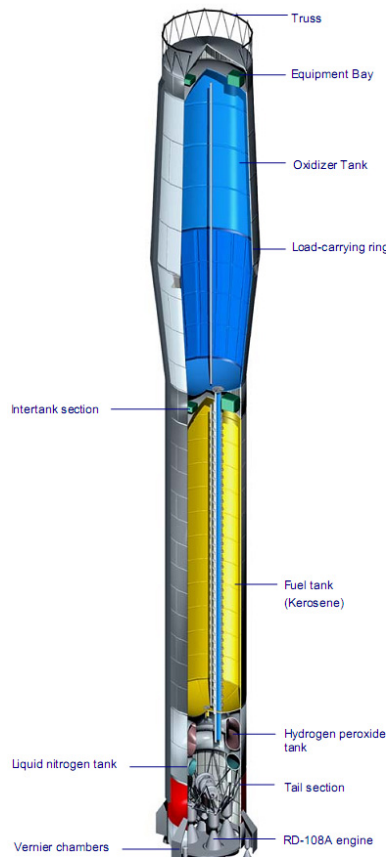


Figure 3: Core stage

<b>Size</b>	2.95m diameter x 27.10m length
<b>Gross/Dry mass</b>	99,765kg / 6,545kg
<b>Propellant</b>	66,800kg LOX 26,300kg Kerosene
<b>Structure</b>	Pressure stabilized aluminium alloy tanks with intertanks skin structure
<b>Propulsion</b>	RD-108A 4-chambers engine
<b>Thrust</b>	792.5kN SL; 990.2kN Vac
<b>Isp</b>	255s – SL; 319s –Vac
<b>Feed system</b>	pump-fed by hydrogen peroxide gas generator
<b>Pressurization</b>	Liquid nitrogen vaporization
<b>Burn time / Restart</b>	286s / No (two level thrust throttling)
<b>Attitude Control</b>	Two 35kN vernier thrusters and one arofin
<b>Avionics</b>	Input/Output units, TM, power
<b>Stage separation:</b>	Pyronuts and 3 <sup>rd</sup> stage ignition

Table 3: Second stage features

both.

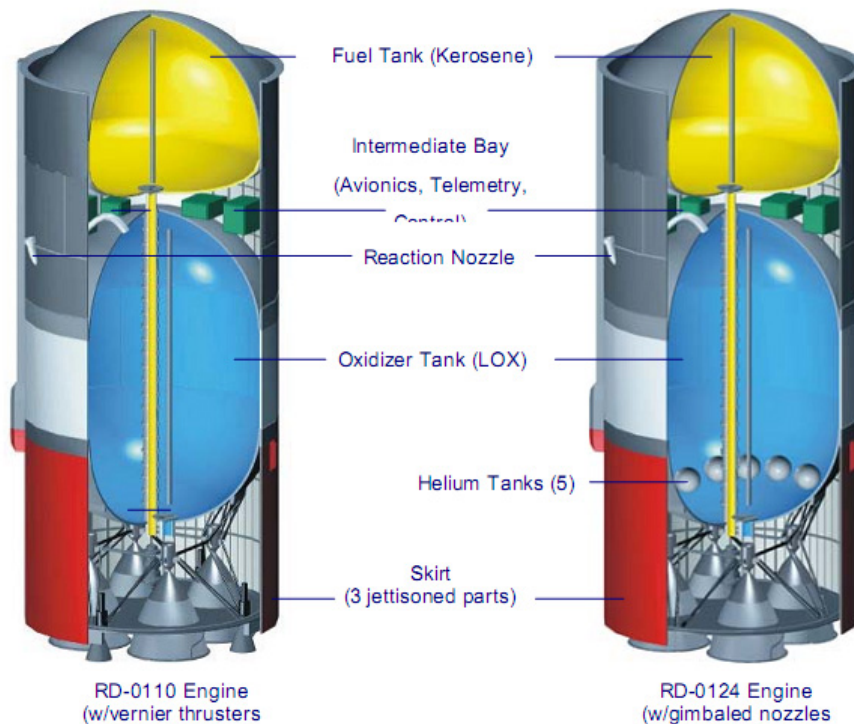


Figure 4: The Block I

The *RD-0110* engine is powered by a single turbopump spun by gas from combustion of the main propellants in a gas generator. These combustion gases are recovered to feed four vernier thrusters that handle attitude control of the vehicle. The LOX tank is pressurized by the heating and evaporation of the oxygen, while the kerosene tank is pressurized by combustion products from the gas generator.

The *RD-0124* engine is a staged combustion engine powered by a multi-stage turbopump spun by gas from combustion of the main propellants in a gas generator. These oxygen rich combustion gases are recovered to feed the four main combustion chambers where kerosene coming from the regenerative cooling circuit is injected. Attitude control is provided by main engine activation along one axis in two planes. LOX and kerosene tanks are pressurized by the heating and evaporation of helium coming from storage vessels located in the LOX tank.

An interstage truss structure connects the core stage with the third stage, thereby allowing for the ignition of the third stage before separation

of the second. In fact, this ignition assists the separation of the second stage.

For de-orbitation and collision avoidance, a reaction nozzle is positioned on the side of the stage and vents the oxygen tank[4].

	<b>RD-0110</b>	<b>RD-0124</b>
<b>Size</b>	2.66m diameter 6.70m length	2.66m diameter 6.70m length
<b>Gross/Dry mass</b>	27,755kg / 2,355kg	27,755kg / 2,355kg
<b>Propellant</b>	17,800kg LOX 7,600kg Kerosene	17,800kg LOX 7,600kg Kerosene
<b>Structure</b>	Pressure stabilized aluminium alloy tanks with intertanks skin structure	Pressure stabilized aluminium alloy tanks with intertanks skin structure
<b>Propulsion</b>	RD-0110 4-chambers engine Soyuz 2-1a	RD-0124 4-chambers engine Soyuz 2-1b
<b>Thrust</b>	297.9kN Vac	297.9kN Vac
<b>Isp</b>	325s Vac	359s Vac
<b>Feed system</b>	Pump-fed gas generator generator's gas blow down through verniers	Multi-stage pump-fed close cycle gas generator
<b>Pressurization</b>	Oxygen vaporization/ generator gases	Helium vaporization
<b>Burn time / Restart</b>	250s / No	270s / No
<b>Attitude Control</b>	Four 6-kN vernier thrusters	Each chambers gimbaling in one axis
<b>Avionics</b>	Centralized control system: inertial 3-axis platform on-board computer TM and RF system, power	Centralized control system: inertial 3-axis platform on-board computer TM and RF system, power

Table 4: Third stage features

#### 2.2.4 The upper stage - Fregat

The *Fregat* (see fig. 5) upper stage is an autonomous and flexible stage designed to operate as an orbital vehicle. It extends the capability of the lower three stages of the Soyuz vehicle to provide access to a full range of orbits.

The upper stage consists of six welded 1.8 mm thick spherical tanks, made of aluminum alloy (AMG-6) (four for propellant, two for avionics) distributed in a circle, with 8 trusses passing through the tanks providing

structural support. The propulsion system consists of a single chamber NTO / UDMH engine capable of in-plane translation, and controlled by electrohydraulic actuators.

In addition to the main engine, Fregat uses twelve thrusters for three-axis attitude control, and for propellant settling before ignition of the main engine. The thrusters are distributed in 4 clusters on the top of the spherical tanks. Up to 85 kg of hydrazine is stored in two tanks dedicated to the ACS.

The three axis inertial measurement unit, the onboard computer and the GPS/GLONASS navigation system form the core of the Fregat control system. The control system is based on a triple-redundant architecture. Both three-axis stabilized orientation and spin-stabilized modes are provided.

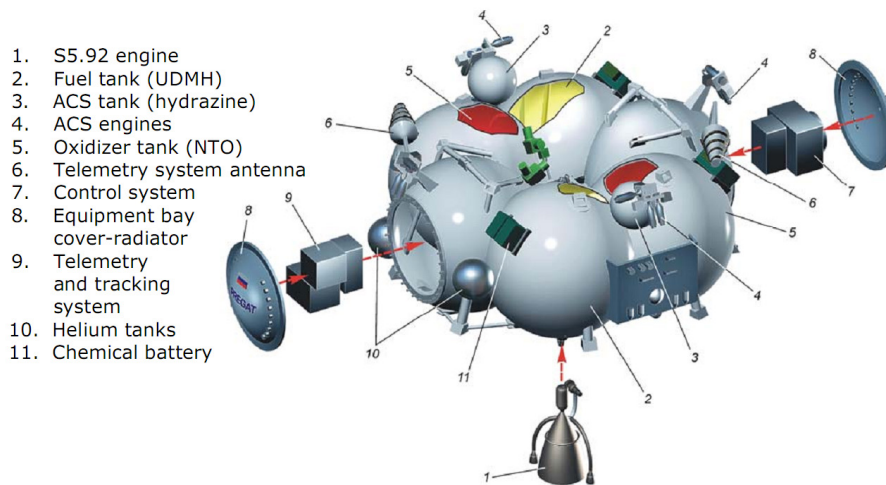


Figure 5: The Fregat

Telemetry system provides transfer of health monitoring data from Fregat to the ground, either via a direct transmission mode or via a playback mode. The S-band transmitter enables communication with CSG ground stations.

The Fregat power supply consists of two Lithium-Chloride batteries. One battery is dedicated to the control system only; the other is dedicated to the remaining equipment. The number of batteries can be increased according to mission duration.

The thermal control system of the two equipment bays consists of two dedicated fans for nitrogen circulation. Thermal insulation and heaters protect the external equipment and the propellant tanks.

The Fregat is a restartable upper stage (main engine with multiple-ignition capability up to 20 times, with six demonstrated during flight), fully independent from the lower composite (IMU, telemetry, power, etc.),

which allows a wide range of missions and even to be potentially compatible with other launch vehicles.

NPO Lavotchkine, is responsible for the production of Fregat. Its facilities can accommodate the production of up to eight upper stages per year with a production time of 10 to 15 months[4].

<b>Size</b>	3.35m diameter x 1.50m height
<b>Inert mass</b>	950 kg
<b>Propellant</b>	5350-kg N <sub>2</sub> O <sub>4</sub> /UDMH
<b>Structure</b>	Structurally stable aluminum alloy 6 spherical tanks/8 cross rods
<b>Propulsion</b>	S5.92
<b>Thrust</b>	Two mode thrust 19.85/14.00kN Vac
<b>Isp</b>	Two mode thrust 331/316s Vac
<b>Feed system</b>	Pump-fed open cycle gas generator
<b>Pressurization</b>	Helium gas vaporization
<b>Burn time / Restart</b>	Up to 900 s / up to 20 controled or depletion burn
<b>Attitude Control - pitch/yaw</b>	Main engine translation or 8 50N hydrazine thrusters
<b>Attitude Control - roll</b>	4 50N hydrazine thrusters
<b>Avionics</b>	Inertial 3-axis platform on-board computer TM and RF systems, Power
<b>Stage separation</b>	gas pressure locks/pushers

Table 5: The upper stage features

#### 2.2.5 Soyuz: a general review

Soyuz medium-lift launcher has had different versions during its long life-time, here it is reported a brief review of its configurations. Some of them have had a more popular life, with a a great number of launch on their credit side, other less.

#### *The Soyuz-U*

*Soyuz-U* (see fig. 6) unified middle-class launch vehicle is intended for injection of Soyuz-type and Progress-type manned and cargo spaceships into near-earth orbit, spacecraft for special purposes (Kosmos-series spacecraft), spacecraft for national economy (Resurs-F-type spacecraft), space-



craft for space technology research and spacecraft for medical and biological purposes (Foton-type and Bion-type spacecraft ), as well as foreign spacecraft. Soyuz-U launch vehicle can be equipped with nose fairing of the following diameters: 2.7m; 3.0m; 3.3m; 3.7m.



Figure 6: The Soyuz-U

In table 6 are reported some of the most important feature of this configuration.

Launch site	Inclination [degree]	Circ. orbit av. altitude [km]	Injected payload [kg]
Plesetsk	62,8	220	6,700
	67,1	190	6,640
	81,4	200	6,200
Baikonur	51,6	200	6,950
	64,9	190	6,660
	70,4	200	6,590

Table 6: Main featurers of Soyuz-U

### *Soyuz-FG*

*Soyuz-FG* (see fig. 7) launch vehicle is intended for injection of automatic spacecraft for national economy, scientific research (Resurs-F1, Resurs-F2, Foton spacecraft) and spacecraft for special purposes (Kosmos-series satellites) as well as manned and cargo spaceships according to the program of the International Space Station.

In contrast to Soyuz-U launch vehicle modernized engines with heightened specific thrust on units of the 1st and the 2nd stages, developed for Soyuz-2 launch vehicle, are used for Soyuz-FG launch vehicle for increasing load-carrying capacity. Soyuz-FG launch vehicle can be equipped with nose fairing of the following diameters: 2.7m; 3.0m; 3.3m; 3.7m.

In table 7 are reported features of payload for this configuration.

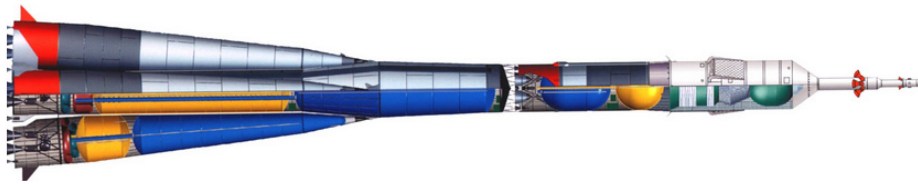


Figure 7: The Soyuz-FG

Launch site	Inclination [degree]	Circ. orbit av. altitude [km]	Injected payload [kg]
Baikonur	51.6	200	7,130
	64.9	190	6,850
	70.4	200	6,790

Table 7: Main features of Soyuz-FG

### *Soyuz-2*

*Soyuz-2* (see fig. 8) launch vehicle is a new launch vehicle. It will enable to replace Soyuz-U, Soyuz-FG and Molniya-M launch vehicles with one launch vehicle in the future. Soyuz-2 launch vehicle with Fregat kick stage will enable to launch spacecrafts to various orbits: low, medium, high elliptical, sun-synchronous, GTO and GSO.

Soyuz-2 launch vehicle has been developed on the basis of Soyuz launch vehicle in two phases (phases 1A and 1B).

Modification phase of *Soyuz-2-1A* launch vehicle:

- injectors with improved mixing characteristics are used in engines of the first and second stages;
- a new control system, unified for three stages, was developed on the basis of highly efficient digital computer;
- a new digital radio-telemetry system is used;
- the third stage unit structure is maximally unified both for modification phase 1A and modification phase 1B.

Modification phase of *Soyuz-2-1B* launch vehicle:

- in addition to improvements of modification phase 1A new engine with greater power capabilities is used in the the third stage unit.

In table 8 are reported some specification for this launcher.

In table 9 are reported some performances for this launcher.



Figure 8: The Soyuz-2

<b>Number of stages</b>	4
<b>Lift-off mass</b>	312tons
<b>Maximal length</b>	46.3m
<b>Nose Fairing diameter</b>	2.7m - 3.0m 3.3m -3.715m -4.11m

Table 8: Specifications of Soyuz-2 launch vehicle

<b>Launch site</b>	<b>Inclination [degree]</b>	<b>Circ. orbit av. altitude [km]</b>	<b>Injected PL Soyuz-2-1A [kg]</b>	<b>Injected PL Soyuz-2-1B [kg]</b>
Plesestk	62.8	220	6,830	7,850
	67.1	190	6,690	7,880
	81.4	200	6,360	7,470
	98.3	200	5,900	6,900
Baikonur	51.6	200	7,020	8,250
	64.9	190	6,710	7,930
	70.4	200	6,660	7,790
	95.4	200	5,500	6,500

Table 9: Power capability of Soyuz-2 launch vehicle

### *Soyuz-ST*

*Soyuz-ST* (see fig. 9) launch vehicle is developed on the bases of Soyuz-2 launch vehicle and design for commercial spacecraft launches from Kourou launching site (French Guiana).

*Soyuz-ST* launch vehicle is adapted in compliance with the requirements of Kourou Space Center in terms of safety (up-link commands to stop the flight), telemetry system (UHF transmitters with European IRIG format for telemetry frame) operational environment (high humidity, sea transportation and others).

*Soyuz-ST* launch vehicle is equipped with ST-type Nose Fairing, meeting international demands. When used with Fregat upper stage it will enable to orbit a wide range of Payloads.

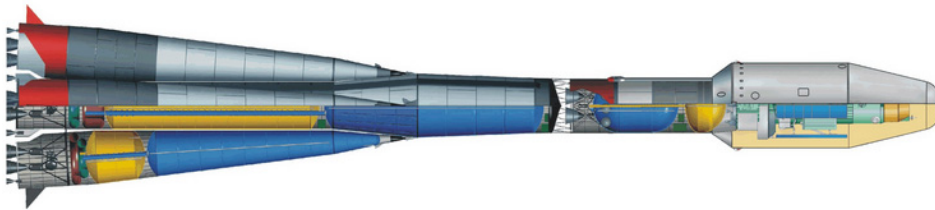


Figure 9: The Soyuz-ST

In table 10 are reported some performances for this launcher.

Launch vehicle	Soyuz-ST-A	Soyuz-ST-B
Geo-transfer orbit	2,850kg	3,240kg
Sun-synchronous orbit	4,230kg	4,900kg

Table 10: Power capacity of Soyuz-ST launch vehicle

### *Soyuz 2-3*

*Soyuz-2-3* launch vehicle is three-stage middle-class launch vehicle, which is an advanced launch vehicle developed on the basis of Soyuz-2 launch vehicle to increase launch vehicle power capacity and expand the range of launched spacecraft.

Gimballed sustainer engine NK – 33 – 1 with upgraded power capability is used in the central module of Soyuz-2-3 launch vehicle.

The bottom part diameter of Soyuz-2-3 launch vehicle central module has been increased from 2,050 up to 2,660mm.

Draft design for Soyuz-2-3 launch vehicle has been developed.

In table 11 are reported some specification for this launcher.

<b>Number of stages</b>	3
<b>Lift-off mass</b>	335.5 – 340tons
<b>Maximal length</b>	47m
<b>Nose Fairing diameter</b>	4.11m

Table 11: Specifications of Soyuz-2-3 launch vehicle

	<b>injected PL [kg]</b>	<b>injected PL [kg]</b>	<b>injected PL [kg]</b>
<b>Launching site</b>	Baikonur	Plesetsk	Kourou
<b>Circular orbit mean altitude ~ 200km</b>	10,000kg (incl. 51.8°)	9,700kg (incl. 62.8°)	10,700kg (incl. 5.3°)
<b>Geo-transfer orbit (with Fregat)</b>	2,480kg	2,100kg	3,900kg
<b>Sun-synchronous orbit (with Fregat)</b>	6,200kg	6,700kg	-

Table 12: Soyuz-2-3 launch vehicle power capacity

## 2.3 PROBLEM OF THE SPACE DEBRIS

As already announced orbital debris is a concerning problem that it started to be more and more on scientists' agenda since the early years of 1990ies. After over 30 years of unregulated exploitation of earth orbit, the situation is evolved in such condition, in which all space agencies, commercial users, and military services, need to stipulate a unified regulatory about launches and launchers, with the aim to have a reduction of new debris generated by new launches, and the mitigation of pollution already present.

NASA, ESA, Roscosmos and IADC (Inter-Agency Space debris Coordination Committee), founded by NASA, ESA, Russian Aviation and space agency and NASDA, have been very useful and active on the promulgation of guidelines for the mitigation/reduction of space pollution. In particular each agency has worked on a modernization and development of new techniques that allow to reduce the quantity of debris generated each launch due to separation of modules, and also systems that allows the removal of spent stages in a disposal orbit or by de-orbiting on earth. Another important theme developed is been the drawing up of a series of laws and a legislation that have to be followed in order to control the orbital environment [5].

Nowadays more than 30,000 objects have been cataloged by the US Space Surveillance Network (SSN), and there is another huge amount

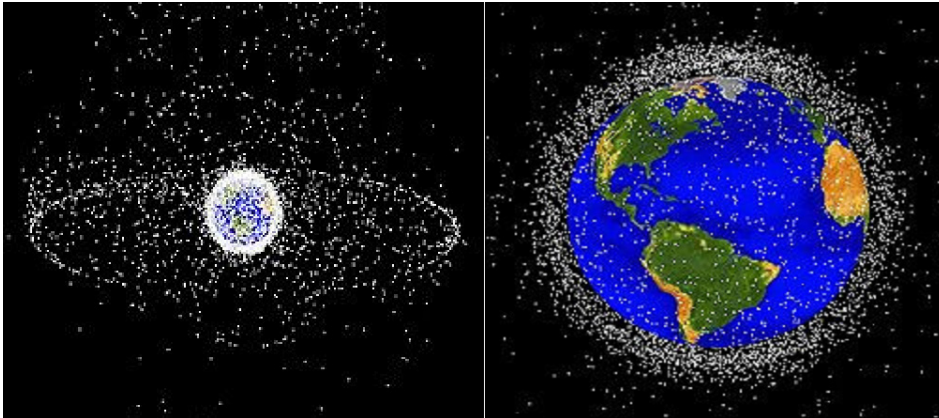


Figure 10: Space debris dispersion

present in orbit that cannot be cataloged due to too little dimensions to be tracked and analyzed. These untrackable objects, that in general consist in bolts, fragments of breakups and pieces left during separation processes are very dangerous because of their unknown trajectories [6].

Pollution Sources	Amount of fragments [%]
In-orbit object fragmentation	46
Spent spacecraft	21
Spent rocket stages	16
Separated elements	11
Operating spacecraft	6

Table 13: Composition of tracked space debris

### 2.3.1 Categories of space debris

During 80ies and 90ies have been made some predictions of the evolution of near-earth debris population on the basis of the object previously cataloged, the expected population has been larger than the real population measured in the 90ies because of the increased solar activity from 1980 till 1992 and the improved technology in launchers[6]. However space debris accumulation is in progress.

Even if its density has not reached a critical level yet, studies conducted by NASA's Orbital Debris Program Office have shown that in the heavily used altitude band (900 – 1000km) the number of fragments larger than 10cm is expected to more the triple over the next 200 years, even assuming no additional objects are launched in that band. These studies also have estimated that the total population of large debris in LEO will increase

by nearly 40% during that time, still under assumption of no additional launches [7].

Space debris can be classified in four classes as it follows[5]:

- **Inactive payloads or inoperative objects:** Inactive payloads are primarily made up of satellites which have run out of fuel for station-keeping operations or have malfunctioned and are no longer able to maneuver. However, the use of the term "inactive payloads" requires clarification. Because satellites can be deactivated for periods of time and then later reactivated, and because debris may include objects manufactured in outer space and not just payloads, the term "inoperative objects" may be more correct when referring to objects which entities can no longer control.
- **Operational debris:** Operational debris includes any intact object or component part that was launched or released into space during normal operations. The largest single category of this type of debris is intact rocket bodies that remain in orbit after launching a satellite.
- **Fragment debris:** Fragmentation debris is created when a space object breaks apart. This type of debris can be created through explosions, collisions, deterioration, or any other means. Some debris have been caused intentionally. The Chinese test is an example but it is not a unique event. For instance, the USSR has intentionally destroyed several reconnaissance satellites to prevent their recovery by other States. In 1985, the US also tested an air launched anti-satellite weapon that produced 230 pieces of trackable debris, and in 1986, intentionally caused two US satellites to collide, producing hundreds more pieces of detectable debris. Collisions are another source of fragmentation debris. Debris of this type may result from collisions between space object and either natural or artificial orbital debris.
- **Microparticulate pattern:** Surface degradation is also a cause of space debris. Surfaces of spacecraft are exposed to the deleterious space environment of ultraviolet radiation, atomic oxygen, thermal cycling, micro-particulates, and micrometeoroids. This can lead to degradation in the optical, thermal and structural integrity of surfaces and coatings with subsequent shedding of materials into the space environment. Indeed, debris can be created as the result of the gradual disintegration of the surfaces on a satellite due to exposure to the space environment.

### 2.3.2 Debris generation: some examples

Briefly it is reported a simple comparison about damaging power of fragments due to their high content of kinetic energy.

Seen that Low Earth Orbit (LEO) is not a limitless resource, it must be managed carefully. Considering that at the orbital velocity of more than 28,000km/h, collisions can be highly damaging to functioning of satellites and spacecraft. At this velocity an object of dimension of 1cm has enough kinetic energy to disable an average-size spacecraft; an object of 1mm of diameter can damage sensitive portions of spacecraft, but these particles are not tracked. At typical impact velocity of 10km/s a droplet of sodium-potassium of 1cm would have the destructive power of a hand grenade. An aluminum sphere of 1.3mm of diameter has damage potential similar to that of a 0.22-caliber long rifle bullet (as a bullet of 40gr at 330m/s). An aluminum sphere of 1cm of diameter is comparable to a safe traveling of about 200kg at a speed of about 100km/h. A fragment which is 10cm in its long dimension is roughly comparable to 25 sticks of dynamite [5].

There have been also some intentional generation of debris, in particular there have been some test of anti-satellite (ASAT) weapon, as in 2007 when China has tested this weapon destroying its defunct weather satellite Feng Yun-1C. By the way in the previous years this kind of weapon has been tested also by Russia and America. The Chinese ASAT test has added some 2000 fragments to the catalog; they make up about 35% of the breakup-debris total. The Soviet ASAT program in the 1970ies and early 1980ies, which attempted to destroy a satellite by shrapnel from an exploding ASAT weapon, created more than 700 pieces of large debris, roughly 300 of which remain in orbit. The last piece of cataloged debris from the one US ASAT test, in september 1985, decayed from orbit in 2004 [7].

Currently the US and Russia are each responsible for about 35% of the cataloged objects in space, and China for about 20% following its ASAT test. The Russian percentage is increased to roughly 40% in the next years after the breakup of Briz-M booster in 2006.

	<b>0.1-1 cm</b>	<b>1-10 cm</b>	<b>&gt;10 cm</b>
<b>Total debris at all altitudes</b>	$150 \cdot 10^6$	$650 \cdot 10^3$	$22 \cdot 10^3$
<b>Debris in LEO</b>	$16 \cdot 10^6$	$270 \cdot 10^3$	$14 \cdot 10^3$
<b>Debris from the breakup of a 5- to 10-tons satellite</b>	$8 - 14 \cdot 10^6$	$150 - 250 \cdot 10^3$	$30 - 50 \cdot 10^3$
<b>Debris from Feng Yun-1C</b>	$2 \cdot 10^6$	$40 \cdot 10^3$	$2 \cdot 10^3$

Table 14: Estimated amount of debris by size



On 11 January 2007 a Chinese ground-based missile was used to destroy the Feng Yun-1C spacecraft, an aging satellite orbiting more than 500 miles in space since May 1999. Although the test was hugely successful from a military point of view, demonstrating China's ability to use very sophisticated weapons to target regions of space that are home to various satellites and space-based systems, it caused great concerns to both the military and scientific communities. Indeed, the event is a real danger in the sense it may fuel an arms race and weaponization of space, with some countries being tempted to show they can easily have a control of space as well. From the scientific perspective, the Chinese destruction of Feng Yun-1C gave a new dimension to the space debris issue.

In shattering the old weather-watching satellite into hundreds of large fragments, the Chinese created a large debris cloud. The debris are now spreading all around the earth, the majority of the them residing in very long-lived orbits. As such, they can seriously damage other satellites in nearby orbit and possibly even spacecraft on their way to the moon or beyond. As of 27 February 2007, the U.S. military's Space Surveillance Network has tracked and cataloged 900 debris fragments greater 5mc, large enough to create potentially serious problems. The total count of objects could go even higher based upon the mass of Feng Yun-1C and the conditions of the breakup, which could have created millions of smaller pieces. The debris cloud extends from less than 200km to more than 3,850km, encompassing all of low Earth orbit [5].

In fig. 11 it is possible to see the evolution of the debris generated after an explosion of an objects presented in orbit, for example it could be the representation of the explosion of Fen Yung-1C.

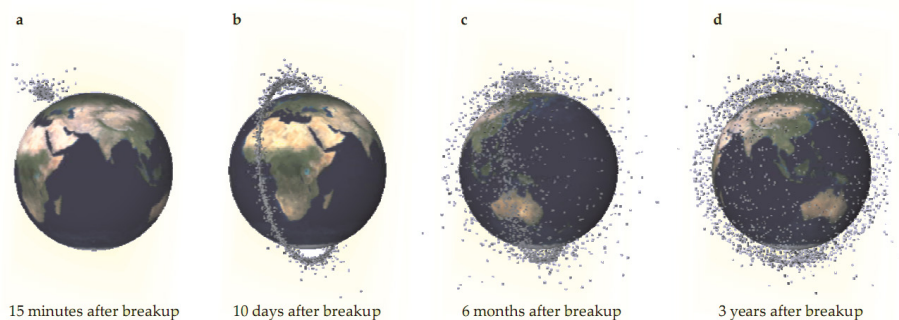


Figure 11: Debris evolution after object explosion

It is possible to understand that also an isolated explosion can affect all near-earth orbit after enough time, that is why the reason of debris mitigation and prevention of explosions is so important. Indeed simulation shows that after 10 days the explosion, fragments are spread for all orbit made by the object, time by time there is a diffusion of fragments

around all near-earth orbit, till reaching a steady state of diffusion where fragments are spread all around earth.

### 2.3.3 *Space debris: sources*

The principal sources of generation of new debris can be different and very variegated. Relying on the analysis of Russian space object fragmentations it is possible to state the following causes as typical ones [8]:

- Explosion of pressurized container enclosing buffer chemical batteries due to the failed charger and depressurization of the batteries (Ekran-2, Kosmos-1275, Kosmos-1823 and other launchers);
- Explosion of the liquid-propellant propulsion system containing unused hypergolic propellant components under long-term space environment effects;
- Modifications of design without scrutinizing their consequences. As an example the vent pipeline mounted in the tail section of the Zenit second stage brought about rotation of the stage's separated part in orbit. The remaining oxygen poured over the oxidizer tank safety valve; as a result the valve was frozen up and when the pressure grew the tank exploded;
- Intended explosions of spacecraft in emergency or explosion for destroying classified information carriers. Made as a rule in LEO with generation of short-lived fragments;
- Proceeding from the analogous reasons and with the aim of preventing space object fragmentation after their active life end all the onboard sources of accumulated energy as well as remaining propellants components, batteries, pressure cylinders, self-destruction appliances, fly wheels and gyroscope must be passivated.

From the first human launch till the present days there have been 186 space object explosions. In table 15 are shown the incidence of each cause.

<b>Fragmentation causes</b>	<b>Explosions number</b>	<b>% value</b>
Propulsion system	58	31
Intended fragmentation	54	29
Unknown reason	51	27.5
Aerodynamic fragmentation	14	7.5
Chemical batteries	8	4.5
Collisions with space debris	1	0.5

Table 15: Percentage incidence of explosions causes

## 2.4 GENERALITIES ABOUT DE-ORBITING SYSTEMS

In order to slow down the production of space debris and try to keep a clean space for the coming generations, several general guidelines have been established. At high level, they are simple and quite self understandable:

- Generation of operational debris shall be avoided, which includes deliberate explosions of course, but also the release of all objects associated to the operations of a space craft;
- Accidental break-ups shall be avoided; to that extent, it is requested to "passivate" the spacecraft or upper stage at the end of its mission, i.e. to get rid of any internal energy stored on board such as propellants, pressurants, electrical energy, etc.
- Two protected orbital regions are defined, from which objects are expected to be removed 25 years after the end of their mission: region A, low Earth orbit (LEO) Region, is the shell surrounding the Earth from ground level to an altitude of 2000 km, where most of the observation satellites are operating; region B, geostationary Earth orbit (GEO) region, is the ring around the GEO, including some margin in altitude and inclination to enable orbital traffic, where most of the communication satellites are located.

These guidelines were formally established and approved unanimously by the 11 Space Agencies composing the Inter Agency Space Debris Co-ordination Committee (IADC) in October 2002; a revised set of guidelines directly inspired from the IADC ones is currently under study at UN level, within the Committee for Peaceful Use of Outer Space (UNCOPUOS). They are also currently being transformed into ISO standards following the efforts of a dedicated international working group [9].

### 2.4.1 *Definition of passivation*

In the IADC guidelines, "passivation" is defined as "the elimination of all stored energy on a space system to reduce the chance of break-up. Typical passivation measures include venting or burning excess propellant, discharging batteries, and relieving pressure vessels". It is important to note that the feared break-up may be either due to internal causes, such as pressure build-up inside propellant tanks following degradation of a thermal protection for instance, or due to external causes such as the impact of a micrometeoroid; in the latter case, the energy released by the collision may be transferred to remaining propellants, leading to an explosive reaction.

The main stored energy sources, which may explode under worst case scenarios, include the following.

- residual propellant in the tanks,
- high pressure gases in pressure vessels (helium tanks),
- overpressure in charged batteries.

Momentum devices such as gyros or wheels also represent an internal energy source, but it can be assumed that their energy level will rapidly decrease when the power is switched off. Heat pipes may certainly be high-pressure devices, but they may usually be left pressurized if the probability of rupture can be demonstrated to be very low. The effect of a potential collision on a heat-pipe has been studied by ESA and tended to show that no significant break-up could be triggered. Namely they should be designed with a sufficient safety margin not to be ruptured by heating after completion of the mission.

Some satellites and most of the upper stages are equipped with command destruct charges for safe reentry, security of data, or other purposes. There has been one documented case of accidental break-up events caused by these devices. Such events can lead to high intensity break-ups with large amounts of debris. The current draft of the ISO standard relative to passivation include some additional sources of energy, such as solar arrays or springs, but they do not really present a credible risk of massive break-up, so they do not have to be taken into account.

As a typical example, the case for Astra 1A may be described; the corresponding definition of passivation and associated sequence of operations was the following: empty the fuel tanks, passivate the batteries and shut off the payload, the attitude control system, the thermal control system, the beacons and telemetry. It led to a perfect disposal, with a final altitude of perigee 440 km above the geostationary orbit, fuel tanks depleted, batteries passivated, solar arrays full Sun and stopped at satellite local noon, all payload transponders off, thermal regulation off, attitude control system off and beacon and telemetry system off [9].

## MISSION ANALYSIS

### 3.1 MISSION PROFILE

In this section is going to be report a typical mission profile for a commercial launch of Soyuz with Fregat as upper stage. A typical mission profile of this launcher can be easily schematized in three phases. In fig. 12 is possible to see the steps and a qualitative mission profile [4].

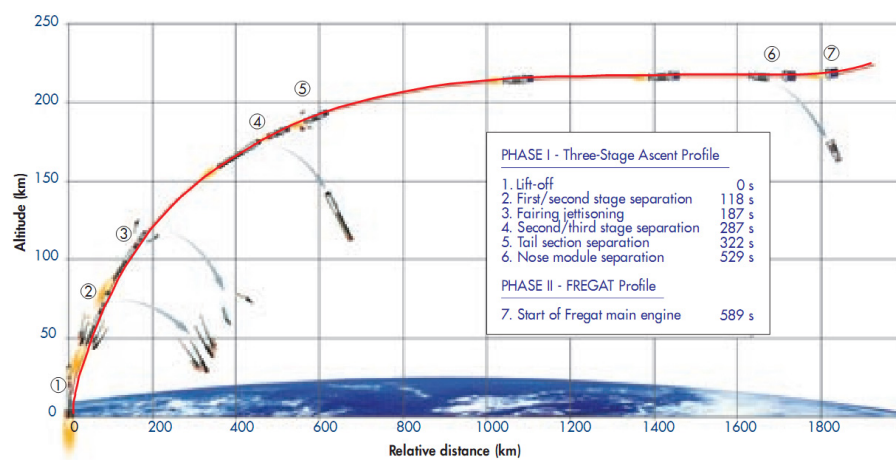


Figure 12: Typical mission profile

The three phases of a typical mission can be summed up in this way:

- **Phase 1:** Lift-off and ascent of the first three stages of the launcher with a suborbital or a direct ascent profile;
- **Phase 2:** Series of orbital maneuvers of Fregat to deliver the payload to final orbit;
- **Phase 3:** Disposal maneuvers or de-orbiting of the upper stage.

#### 3.1.1 Phase 1

The suborbital injection profile separates the third stage and the Fregat at less than orbital velocity, causing the third stage to fall immediately back to earth. The Fregat is then used to reach the first parking orbit. By injecting the entire third stage into orbit along with the Fregat and payload, the direct ascent profile results in slightly lower performance in

comparison to most missions. Generally, the direct ascent profile is used for escape missions with hyperbolic excess (escape) velocities greater than 5.0 km/s.

Jettisoning of the payload fairing can take place at different times depending on the aero-thermal flux requirements on the payload. Typically, fairing separation takes place between 155 and 200 seconds from liftoff owing to aero-thermal flux limitations. If required, the Soyuz/ST can perform an out-of-plane yaw-steering maneuver during third-stage flight in order to change inclination from the nominal value resulting from a direct ascent on the authorized launch azimuth or to compensate for launch-time delay.

The Fregat and its attached payload are separated approximately 520 – 530 seconds following liftoff. The third stage discarded from the flight path falls back to earth in an authorized third-stage drop area. A specific third-stage drop area will be allocated for each mission and in most cases will be located in the ocean. The drop area will be analyzed during the project, especially when dogleg maneuvers are to be incorporated [4].

Here are reported some of the main trajectory parameters relative of the ascent of the first three stages.

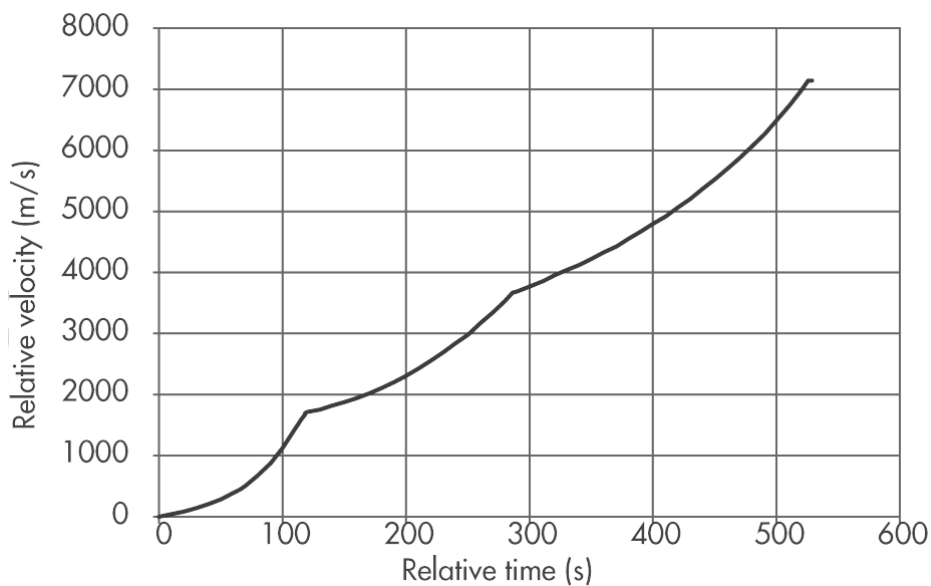


Figure 13: Velocity profile

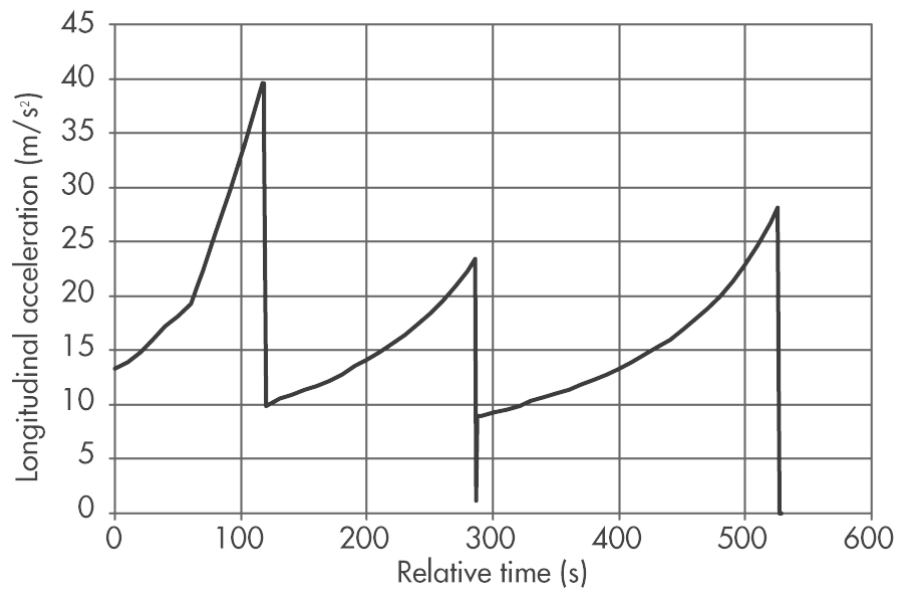


Figure 14: Acceleration profile

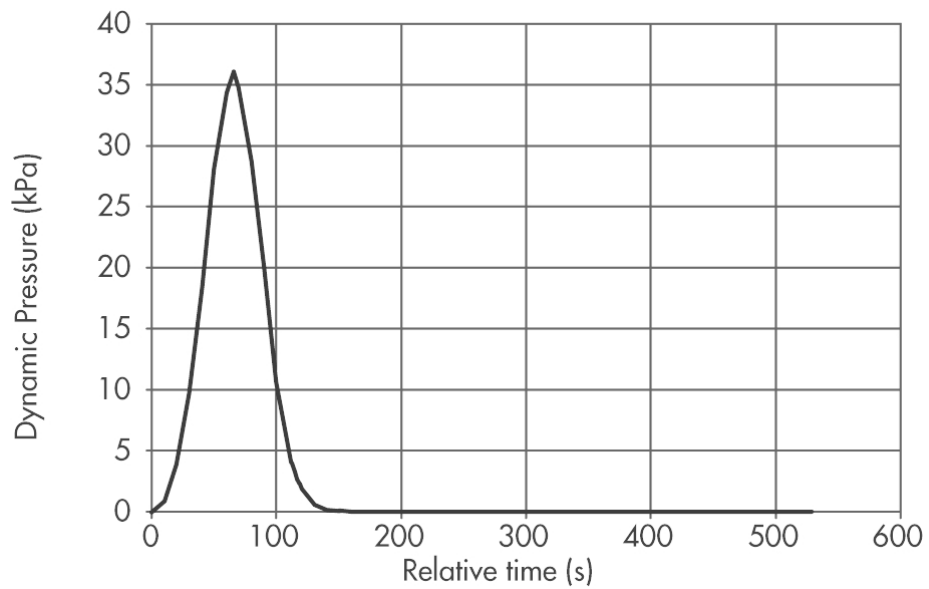


Figure 15: Dynamic pressure profile

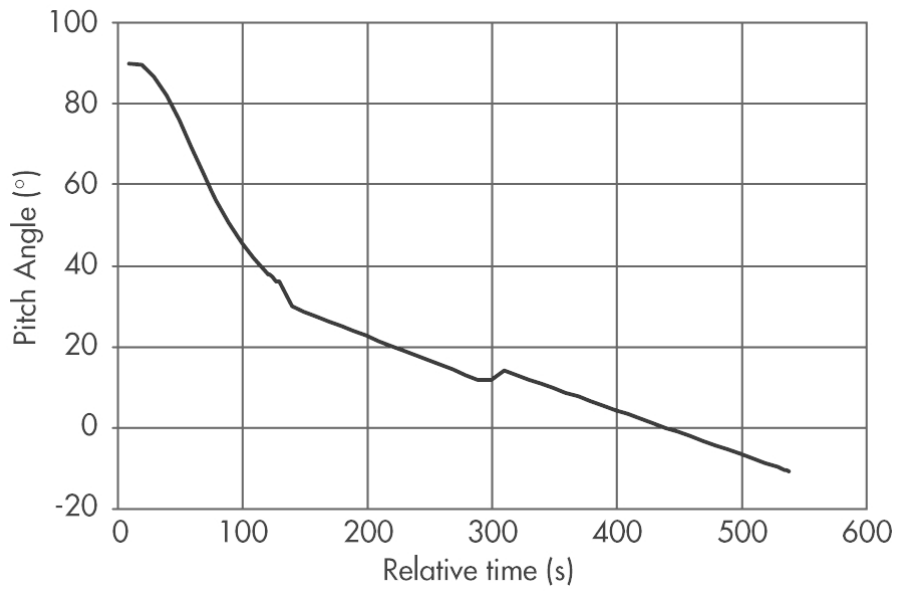


Figure 16: Pitch angle profile

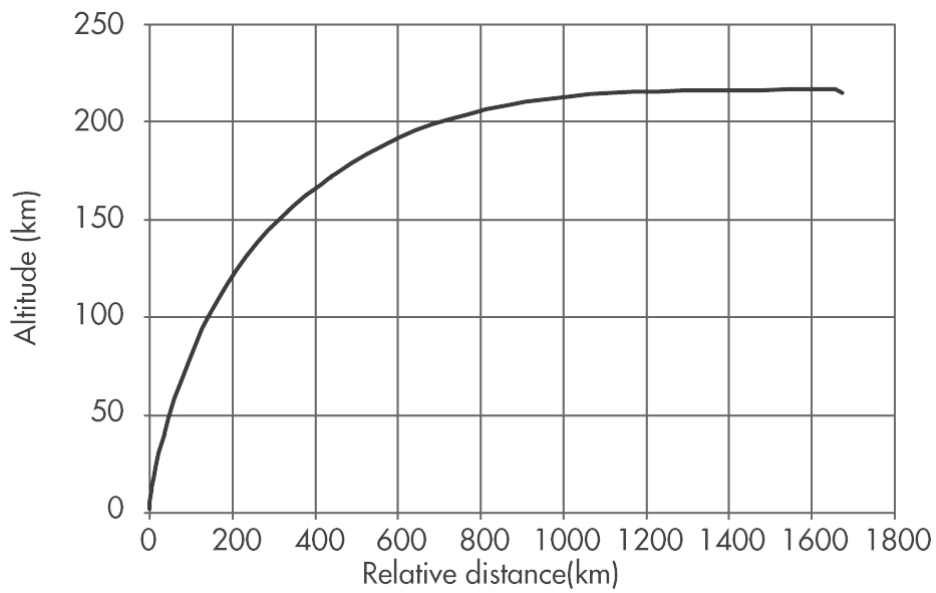


Figure 17: Altitude versus distance profile



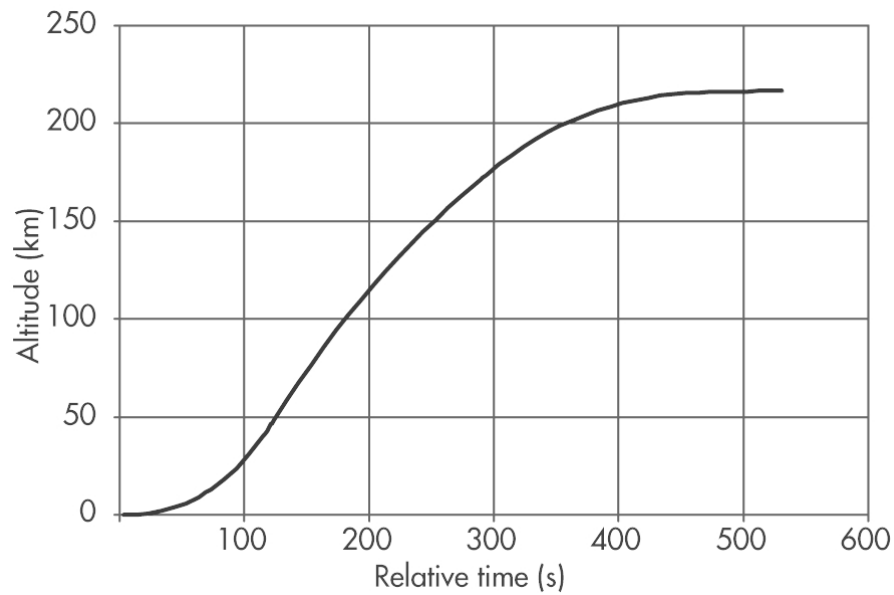


Figure 18: Altitude versus time profile

### 3.1.2 *Phase 2*

Following the cutoff of the third stage, the restartable Fregat upper stage completes the job of delivering the payload or payloads to their final orbits. This profile consists of the following events:

- The ACS thrusters start 5 seconds after separation from the third stage;
- 55 seconds later, the Fregat's main engine is started to transfer to a 200-km parking orbit;
- Following the initial parking orbit, the Fregat is used to transfer the payload to a wide variety of orbits, providing plane change and orbit raising.

Up to 20 burns may be provided by the Fregat to reach the final orbit or to arrange the payload among different orbits [4].

### 3.1.3 *Phase 3*

After spacecraft separation and following the time delay needed to provide a safe distance between the Fregat upper stage and the spacecraft, the Fregat typically conducts a de-orbitation or orbit disposal maneuver. Usually, this maneuver will be carried out by an additional burn of the Fregat's ACS thrusters. Parameters of the "safe" orbit or entry into the

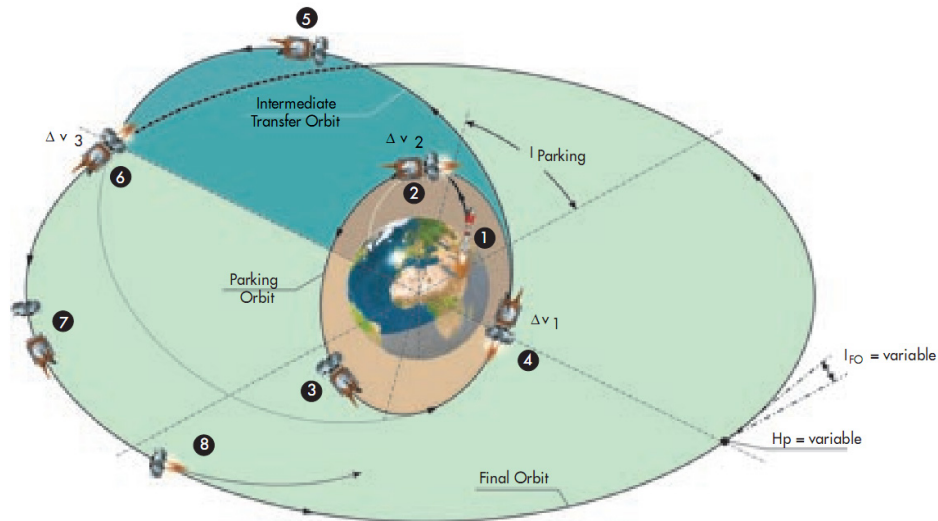


Figure 19: Upper stage typical profile

earth's atmosphere will be chosen in accordance with international laws pertaining to space debris and will be coordinated with the user during mission analysis [4].

### 3.2 DE-ORBITING MISSION PROFILE

The first and the second stages do not need any system which produce any thrust useful to de-orbit them. Seen that these components reach very low altitude and do not have great kinetic energy have, it is not necessary to develop a system dedicated to the de-orbiting maneuver because they fall on earth by their own under the action of gravity and atmospheric drag. The upper stage is already equipped with a de-orbiting system which start working after having left on working orbit the payload.

Depending of the type of mission and the trajectory chosen, the Block I may have enough energy not to de-orbit immediatly, so it could become useful to supply it with an on-board de-orbiting system (*ADOS*). This kind of system is handy for different reasons, mainly for:

- debris removal;
- falling site variation.

In this work the attention is focused on the development of an on-board de-orbiting system for the Block I. Assuming that the orbit of Block I is a circular orbit at the altitude of 220km, the ideal  $\Delta v$  that the system should give to have an immediate reentry on earth will be obtained as follow.

The circular orbit velocity " $v_{\text{circ}}$ " for a given altitude is:

$$v_{\text{circ}} = \sqrt{\frac{G(M+m)}{R}} \approx \sqrt{\frac{G \cdot M}{R}} = \sqrt{\frac{\mu}{R}} \quad (3.1)$$

$$v_{\text{circ}} = \sqrt{\frac{4.32 \cdot 10^{14} [\text{m}^3/\text{s}^2]}{(6.374 + .220) \cdot 10^6 [\text{m}]} = 8,094.1 \left[ \frac{\text{m}}{\text{s}} \right]}$$

where " $G$ " is the gravitational constant, " $M$ " is the mass of the earth, " $m$ " is the mass of the Block I ( $\approx 0$ ), " $\mu$ " the standard gravitational parameter and " $R$ " is the radius of the earth plus the orbit altitude.

The eccentricity " $e$ " of the trajectory is:

$$\frac{H}{R_E} = \frac{e}{1-e} \left( 1 - \cos \left( \frac{\Phi}{2} \right) \right) \quad (3.2)$$

$$e = \frac{\frac{H}{R_E}}{\frac{H}{R_E} + (1 - \cos(\frac{\Phi}{2}))} = 0.1054$$

where " $H$ " is the altitude of the orbit (220 km), " $R_E$ " is the radius of earth, " $\Phi$ " is assumed at  $90^\circ$ .

From eq.3.2 is possible to evaluate the apogee of the trajectory:

$$\frac{a}{R_E} = \frac{1 - e \cdot \cos(\frac{\Phi}{2})}{1 - e^2} \quad (3.3)$$

$$a = 5.9652 \cdot 10^6 [\text{m}]$$

To evaluate the operative velocity  $v_{\text{op}}$ :

$$v_{\text{op}} = \left( \frac{\mu \cdot (1 - e)}{a \cdot (1 + e)} \right)^{1/2} \quad (3.4)$$

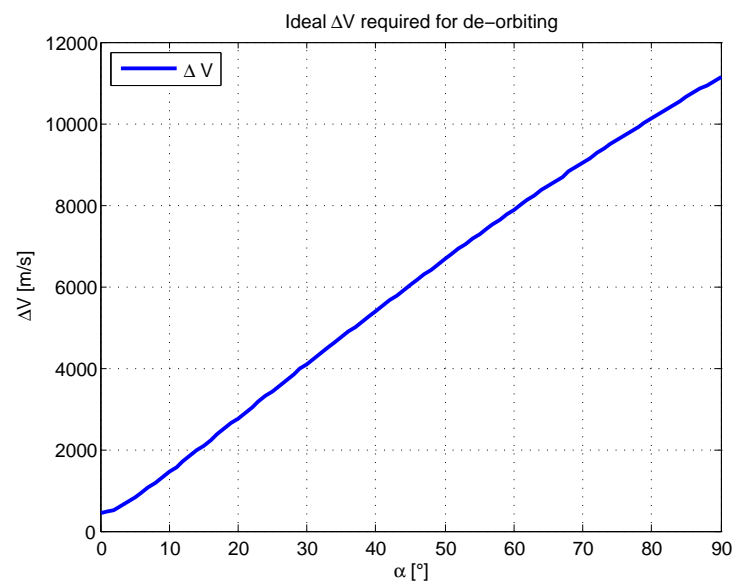
$$v_{\text{op}} = \left( \frac{4.32 \cdot 10^{14} \cdot (1 - 0.1054) [\text{m}^3/\text{s}^2]}{5.9652 \cdot 10^6 \cdot (1 + 0.1054) [\text{m}]} \right)^{1/2} = 7,665.7 [\text{m}/\text{s}]$$

Whence the decrease necessary to give to obtain the de-orbiting maneuver is:

$$\Delta v = \sqrt{v_{\text{circ}}^2 + v_{\text{op}}^2 - 2 \cdot v_{\text{circ}} \cdot v_{\text{op}} \cdot \cos(\alpha)} \quad (3.5)$$

In the fig. 20 is reported the trend of " $\Delta v$ " versus " $\alpha$ ".

Where the minimum  $\Delta v$  required is when  $\alpha = 0$ , that values  $\Delta v = 438.4 [\text{m}/\text{s}]$ .

Figure 20:  $\Delta v$  versus  $\alpha$

## DESCRIPTION OF THE PROBLEM

---

### 4.1 DESCRIPTION OF THE PROBLEM

At the end of its mission in tanks of the Block I is left a certain amount of unused propellant, typically is estimated in the 3% of the initial propellant mass.

To generate a thrust with which is possible to return in earth atmosphere it has been thought to exploit as more as possible the residual energy contained in tanks, through the evaporation of the unused RP – 1 and LOX. This process of gasification is made by introducing in tanks a mass flow of warm gases at the max temperature of 900K, generated by a gas generator. These warm gases interact with the gas of pressurization present in tanks, fuel and oxidizer heating them. In this way the mean temperature of gas increase and there is a heat exchange between gas and liquid. The temperature of liquid increase till reaching the boiling point, and thus the evaporation has its climax.

The initial condition are the following:

- initial pressure of fuel tank: 3.2atm
- initial pressure of oxidizer tank: 1.2atm
- initial temperature of pressurization gas: 150K
- initial temperature of fuel (RP – 1): 288K
- initial temperature of combustible (LOX): 92K

The maximum pressure that tanks could reach is of 5atm.

To develop the analytic model that allows a better comprehension of the phenomena is been made some hypothesis in modeling the condition inside the tanks. It is been assumed an unused mass of 3% (made up by 3% of oxidizer total mass and 3% of fuel total mass). This value has a great level of uncertainty because of some reasons such as: not symmetric working conditions of the valves of fuel and oxidizer tanks, mixture ratio different from the project value, conditions of lack of gravity that allows the formation of liquid bubbles, working conditions of the pressurization system different from the project. These are the main and most remarkable reason why it is impossible to understand the correct condition of tanks when it is necessary to start the de-orbiting maneuver.

## 4.2 DESCRIPTION OF COMPONENTS

Principal features of RP – 1 and LOX are reported in the following paragraphs.

### 4.2.1 *RP-1*

RP-1 (alternately, Rocket Propellant-1 or Refined Petroleum-1) is a highly refined form of kerosene outwardly similar to jet fuel, used as a rocket fuel. Although having a lower specific impulse than liquid hydrogen (LH<sub>2</sub>), RP-1 is cheaper, can be stored at room temperature, is far less of an explosive hazard and is far denser. By volume, RP-1 is significantly more powerful than LH<sub>2</sub> and LOX/RP-1 has a much better ISP-density than LOX/LH<sub>2</sub>. RP-1 also has a fraction of the toxicity and carcinogenic hazards of hydrazine, another room-temperature liquid fuel. Thus, kerosene fuels are more practical for many uses.

RP-1 is most commonly burned with LOX (liquid oxygen) as the oxidizer, though other oxidizers have also been used. RP-1 is a fuel in the first-stage boosters of the Soyuz-FG, Energia, Delta I-III and Atlas rockets. It also powered the first stages of the Soyuz-FG, Titan I, Saturn I and IB, and Saturn V.

During and immediately after World War II, alcohols (primarily ethyl alcohol, occasionally methyl alcohol) were the single most common fuel for large liquid-fueled rockets. Its high heat of vaporization kept regeneratively cooled engines from melting, especially considering that alcohols would typically contain several percent water. However, it was recognized that hydrocarbon fuels would increase engine efficiency, due to a slightly higher density, the lack of an oxygen atom in the fuel molecule, and negligible water content. Whatever hydrocarbon was chosen, though, would have to replicate alcohol's coolant ability.

Many early rockets had burned kerosene, but as burn times, combustion efficiencies, and combustion-chamber pressures grew, and as engine masses shrank, the engine temperatures became unmanageable. Raw kerosene used as coolant would dissociate and polymerize. Lightweight products in the form of gas bubbles, and heavy ones in the form of engine deposits, then blocked the narrow cooling passages. The coolant starvation raised temperatures further, accelerating breakdown. This cycle would escalate rapidly (i.e., thermal runaway would occur) until an engine wall ruptured.

This occurred even with the entire flow of kerosene used as coolant. Rocket designers turned to the fuel chemists to formulate a heat-resistant hydrocarbon. The specification was completed in the mid-50s.

First, sulfur compounds were severely restricted. Small amounts of sulfur are naturally present in fossil fuels. It had already been known that sulfur and sulfur compounds attack metals at high temperatures. In addition, even small amounts of sulfur will assist polymerization.

Alkenes and aromatics were held to very low levels. These unsaturated hydrocarbons tend to polymerize not only at temperature, but during long periods of storage. At the time, it was thought that kerosene-fueled missiles might remain in storage for years awaiting activation. This function was later transferred to solid-fuel rockets, though the high-temperature benefits of saturated hydrocarbons remained. Because of the low alkenes and aromatics, RP-1 is less toxic than various jet and diesel fuels, and far less toxic than gasoline.

The more desirable isomers were selected or synthesized. Linear alkanes were removed in favor of highly branched and cyclic molecules. This increased resistance to thermal breakdown, much as these isomer types improve octane rating in piston engines. Jet engines and heating and lighting applications, the prior users of kerosene, had been much less concerned with thermal breakdown and isomer contents. The most desirable isomers were polycyclics, loosely resembling ladderanes.

In production, these grades were processed tightly to remove impurities and side fractions. Ashes were feared likely to block fuel lines and engine passages, as well as wear away valves and turbo-pump bearings which were lubricated by the fuel itself. Slightly too-heavy or too-light fractions affected lubrication abilities, and were likely to separate during storage and under load. The remaining hydrocarbons are at or near  $C_{12}$  weight. Because of the lack of light hydrocarbons, RP-1 has a high flash point, and is less of a fire hazard than gasoline/petrol or even some jet and diesel fuels.

All told, the final product is more expensive than straight-run kerosene. On paper, any petroleum can produce some RP-1 with enough processing. In practice, the fuel is sourced from a small number of oil fields with high-quality base stock. This, coupled with small demand in a niche market compared to other petroleum users, drives the price. Military specifications of RP-1 are covered in MIL-R-25576 and some chemical and physical properties of RP-1 and RP-2 are tabulated here. Soviet and Russian rocket-grade kerosenes are very similar to RP-1 and are designated T-1 and RG-1. Densities are higher, 0.82 to 0.85 g/ml, compared to RP-1 at 0.81 g/ml. For a short period, the Soviets achieved even higher densities by super-chilling the kerosene in a rocket's fuel tanks, but this partially defeated the purpose of using kerosene over other super-chilled fuels. In the case of the Soyuz and other R7-based rockets, the temperature penalty was minor. Facilities were already in place to manage the vehicle's cryogenic liquid oxygen and liquid nitrogen, both of which are far colder than the kerosene temperature. The launcher's central kerosene

tank is surrounded on four sides and the top by liquid oxygen tanks; the liquid nitrogen tank is nearby at the bottom. The kerosene tanks of the four boosters are relatively small and compact, and also between a liquid oxygen and a liquid nitrogen tank. Thus, once the kerosene was chilled initially, it could remain so for the brief time needed to finish launch preparations.

Chemically, a hydrocarbon propellant will be less efficient than hydrogen fuel. Hydrogen is the lightest molecule; when combusted with oxygen, the  $H_2O$  product has a low weight, and thus a high exhaust velocity. Hydrogen engines are operated fuel-rich, so some exhaust is unreacted  $H_2$ , which is even lighter. Hydrocarbons, on the other hand, produce both  $H_2O$  and  $CO_2$ .  $CO_2$  is over 2.5 times heavier, slowing the exhaust. It can also absorb significant amounts of combustion energy by generating any of several oscillating modes between the atoms. This is energy that could have instead gone into exhaust velocity, and thus, thrust. The heavier oxygen atoms absorb much more energy than the two hydrogens of  $H_2O$ . American designed hydrocarbon engines are also run fuel-rich, which produces some  $CO$  instead of  $CO_2$ . But this also results in incomplete combustion, producing some organics of high molecular weight and numerous vibration modes. All told, kerosene engines generate an  $I_{sp}$  in the range of 270 to 360 seconds, while hydrogen engines achieve 370–465 seconds.

During engine shutdown, fuel flow goes to zero rapidly, while the engine is still quite hot. Residual and trapped fuel can polymerize or even carbonize at hot spots or in hot components. Even without hot spots, heavy fuels can create a petroleum residue, as can be seen in gasoline, diesel, or jet fuel tanks that have been in service for years. Rocket engines have cycle lifetimes measured in minutes or even seconds, preventing truly heavy deposits. However, rockets are much more sensitive to a deposit, as described above. Thus, kerosene systems generally entail more tear downs and overhauls, creating operations and labor expenses. This is a problem for expendable engines as well as reusable ones, because engines must be ground-fired some number of times beforehand. Even cold-flow tests, in which the propellants are not ignited, can leave residues.

On the upside, kerosene below a chamber pressure about 1000 psi can produce sooty deposits on the inside of the nozzle and chamber liner. This acts as a significant insulation layer, and can reduce the heat flow into the wall by roughly a factor of two.

Recent heavy-hydrocarbon engines have modified components and new operating cycles, in attempts to better manage leftover fuel, achieve a more-gradual cool down, or both. This still leaves the problem of non-dissociated petroleum residue. Other new engines have tried to bypass



the problem entirely, by switching to light hydrocarbons such as methane or propane gas. Both are volatiles, so engine residues simply evaporate. If necessary, solvents or other purgatives can be run through the engine to finish dispersion. The short-chain carbon backbone of propane (a 3C molecule) is very difficult to break; methane, with a single carbon atom (1C), is technically not a chain at all. The breakdown products of both molecules are also gases, with fewer problems due to phase separation, and much less likelihood of polymerization and deposition. However, methane (and to a lesser extent propane) reintroduces handling inconveniences that prompted kerosenes in the first place. The low vapor pressure of kerosenes gives safety for ground crews. However, in flight the kerosene tank will need a separate system of pressurization, to replace fuel volume as it drains. Generally, this is a separate tank of liquid or high-pressure inert gas, such as nitrogen or helium. This creates extra cost and weight. Cryogenic or volatile propellants generally do not need a separate pressurant; instead, some propellant is expanded (often with engine heat) into low-density gas, and routed back to its tank. A few highly-volatile propellant designs do not even need the gas loop; some of the liquid automatically vaporizes to fill its own container. Some rockets use gas from a gas generator to pressurize the fuel tank; usually, this is exhaust from a turbo-pump. Although this saves the weight of a separate gas system, the loop now has to handle a hot, reactive gas instead of a cool, inert one.

Regardless of chemical constraints, RP-1 has supply constraints, due to the very small size of the launch-vehicle industry versus other consumers of petroleum. While the material price of such a highly-refined hydrocarbon is still less than many other rocket propellants, the number of RP-1 suppliers is limited. A few engines have attempted to use more standard, wide-distribution petroleum products such as jet fuel or even diesel. By using alternate or supplemental engine cooling methods, some can tolerate the non-optimal formulations.

Any hydrocarbon-based fuel when burned produces more air pollution than hydrogen. Hydrocarbon combustion produces carbon dioxide (CO<sub>2</sub>, a greenhouse gas), toxic carbon monoxide (CO), hydrocarbon (HC) emissions, and oxides of nitrogen (NO<sub>x</sub>), while hydrogen (H<sub>2</sub>) reacts with oxygen (O<sub>2</sub>) to produce only water (H<sub>2</sub>O), with some unreacted H<sub>2</sub> also released.

RP-1 can be compared to Dodecane (fig.21) C<sub>12</sub>H<sub>26</sub> for its characteristics. RP-1 and its evaporation's compound properties are reported in table ?? [1].

Dodecane is a liquid alkane hydrocarbon with the chemical formula CH<sub>3</sub>(CH<sub>2</sub>)<sub>10</sub>CH<sub>3</sub> (or C<sub>12</sub>H<sub>26</sub>), an oily liquid of the paraffin series. It has 355 isomers. It is used as a solvent, distillation chaser, scintillator component. The combustion reaction is:

	$M_m$ [ $\frac{g}{mol}$ ]	$T_b$ [K]	$T_c$ [k]	$P_c$ [bar]	$V_c$ [ $\frac{cm^3}{mol}$ ]	$Z_c$	$\omega$
RP-1	$\sim 175$	420-460	562.7	17.80	707.5	0.2454	0.5703
Dodecane	170.34	489.5	658.2	18.2	713	0.24	0.575
Propane	44.094	231.1	369.8	42.5	203	0.281	0.153
2-methylbutane	72.152	301.0	460.4	33.9	306	0.271	0.227
2-methylpentane	86.178	333.4	497.5	30.2	367	0.267	0.278
n-hexane	86.178	341.9	507.5	30.1	370	0.264	0.299
benzene	78.114	353.2	562.2	48.9	259	0.271	0.212
methylcyclopentane	86.162	345.0	532.7	37.8	319	0.272	0.231
n-heptane	100.205	371.6	540.3	27.4	432	0.263	0.349
1,3-dimethylcyclopentane	98.189	361.0	547	34.4	360	0.27	0.273
methylcyclohexane	98.189	374.1	572.2	34.7	368	0.268	0.236

Table 16: RP-1 and compounds properties [1]

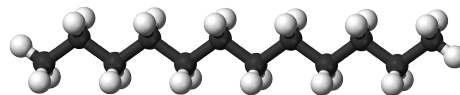
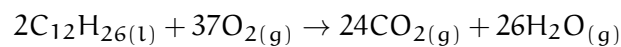


Figure 21: Dodecane molecular structure



If we consider the process of evaporation of RP-1, we must consider that  $CH_{1.935}$  does not evaporate as a singular molecule, but there is a decomposition of it in more volatile components [2] presented in table 17.

#### *Evaporation's compounds*

**PROPANE** Propane (fig.22) is a three-carbon alkane, normally a gas, but compressible to a transportable liquid. A by-product of natural gas processing and petroleum refining, it is commonly used as a fuel for engines, oxy-gas torches, barbecues, portable stoves and residential central heating.

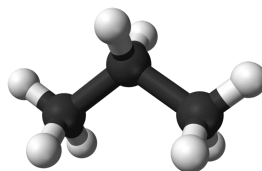


Figure 22: Propane molecular structure

compound	mass %
propane	46.7
2-methylbutane	24.9
2-methylpentane	7.8
n-hexane	7.7
benzene	3.7
methylcyclopentane	3.4
n-heptane	1.8
1,3-dimethylcyclopentane	1.4
methylcyclohexane	1.4
toluene	1.2

Table 17: RP-1 evaporation components [2]

Propane undergoes combustion reactions in a similar fashion to other alkanes. In the presence of excess oxygen, propane burns to form water and carbon dioxide.



**2-METHYLBUTANE** Isopentane (fig. 23),  $\text{C}_5\text{H}_{12}$ , also called methylbutane or 2-methylbutane, is a branched-chain alkane with five carbon atoms. Isopentane is an extremely volatile and extremely flammable liquid at room temperature and pressure. The normal boiling point is just a few degrees above room temperature and isopentane will readily boil and evaporate away on a warm day. Isopentane is commonly used in conjunction with liquid nitrogen to achieve a liquid bath temperature of  $-160^\circ\text{C}$

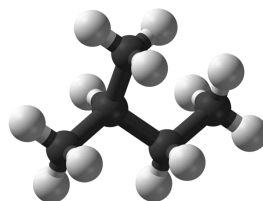


Figure 23: Isopentane molecular structure

**2-METHYLPENTANE** 2-Methylpentane is a branched-chain alkane with the molecular formula  $\text{C}_6\text{H}_{14}$ . It is a structural isomer of hexane composed of a methyl group bonded to the second carbon atom in a pentane chain. It is of similar structure to one of its isomers, 3-methylpentane, which has the methyl group located on the third carbon of the pentane chain.

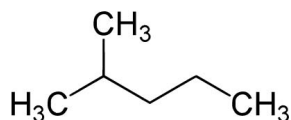


Figure 24: Isohexane molecular structure

**N-HEXANE** Hexane is a hydrocarbon with the chemical formula  $C_6H_{14}$ ; that is, an alkane with six carbon atoms. The term may refer to any of four other structural isomers with that formula, or to a mixture of them. In the IUPAC nomenclature, however, hexane is the unbranched isomer (n-hexane); the other four structures are named as methylated derivatives of pentane and butane. IUPAC also uses the term as the root of many compounds with a linear six-carbon backbone, such as 2-methylhexane  $C_7H_{16}$ , which is also called 'isoheptane'. Hexanes are significant constituents of gasoline. They are all colorless liquids at room temperature, with boiling points between 50 and 70 °C, with gasoline-like odor. They are widely used as cheap, relatively safe, largely unreactive, and easily evaporated non-polar solvents.

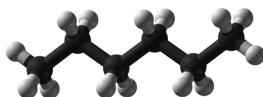


Figure 25: n-Hexane molecular structure

**BENZENE** Benzene is an organic chemical compound with the molecular formula  $C_6H_6$ . It is sometimes abbreviated Ph-H. Benzene is a colorless and highly flammable liquid with a sweet smell. Because it is a known carcinogen, its use as an additive in gasoline is now limited, but it is an important industrial solvent and precursor in the production of drugs, plastics, synthetic rubber, and dyes. Benzene is a natural constituent of crude oil, and may be synthesized from other compounds present in petroleum. Benzene is an aromatic hydrocarbon and the second [n] – annulene ([6] – annulene), a cyclic hydrocarbon with a continuous pi bond. It is also related to the functional group arene which is a generalized structure of benzene.

**METHYLCYCLOPENTANE** Methylcyclopentane is an organic compound with the chemical formula  $CH_3C_5H_9$ . It is one of the important benzene precursors that can react in refinery processes to form benzene.

**N-HEPTANE** n-Heptane is the straight-chain alkane with the chemical formula  $H_3C(CH_2)_5CH_3$  or  $C_7H_{16}$ . When used as a test fuel component

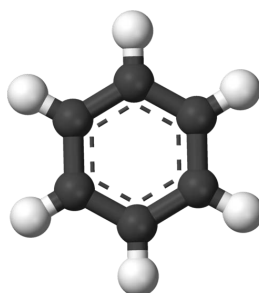


Figure 26: Benzene molecular structure

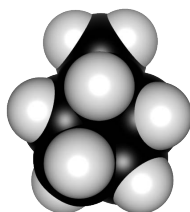


Figure 27: Methylcyclopentane molecular structure

in anti-knock test engines, a 100% heptane fuel is the zero point of the octane rating scale (the 100 point is a 100% iso-octane). Octane number equates to the anti-knock qualities of a comparison mixture of heptane and isooctane which is expressed as the percentage of isooctane in heptane and is listed on pumps for gasoline dispensed in the United States and internationally.

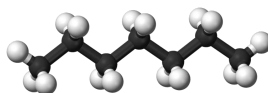


Figure 28: n-Heptane molecular structure

**1,3-DIMETHYLCYCLOPENTANE** 1,3-dimethylcyclopentane is a liquid colorless hydrocarbon with the chemical formula  $C_7H_{14}$ .

**METHYLCYCLOHEXANE** Methylcyclohexane is a colourless liquid with a faint benzene-like odor. Its molecular formula is  $C_7H_{14}$ . Methylcyclohexane is used in organic synthesis and as a solvent for cellulose ethers. It is a component of jet fuel and is also a component of correction fluids

**TOLUENE** Toluene, formerly known as toluol, is a clear, water-insoluble liquid with the typical smell of paint thinners. Chemically it is a mono-substituted benzene derivative, i.e. one in which a single hydrogen atom

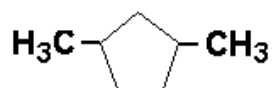


Figure 29: 1,3-dimethylcyclopentane molecular structure

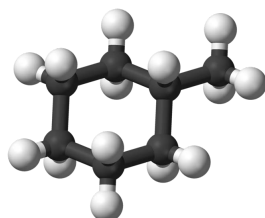


Figure 30: Methylcyclohexane molecular structure

from the benzene molecule has been replaced by a univalent group, in this case CH<sub>3</sub>. It is an aromatic hydrocarbon that is widely used as an industrial feedstock and as a solvent. Like other solvents, toluene is sometimes also used as an inhalant drug for its intoxicating properties; however, this can potentially cause severe neurological harm.

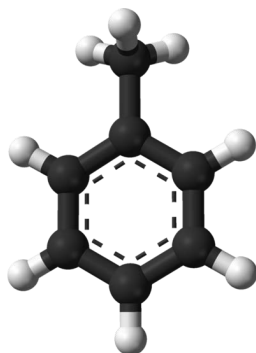


Figure 31: Toluene molecular structure

#### 4.2.2 *Liquid oxygen*

Liquid oxygen, often abbreviated as LOX, boils at 92 K at atmospheric pressure; at these conditions it has a specific gravity of 1.14 kg/m<sup>3</sup> and a heat of vaporization of 213 kJ/kg. It is widely used as an oxidizer and burns with a bright white-yellow flame with most hydrocarbon fuels. It has been used in combination with alcohols, jet fuels (kerosene-type), gasoline, and hydrogen. As shown in table 18, the attainable performance

is relatively high, and liquid oxygen is therefore a desirable and commonly used propellant in large rocket engines.

The following missiles and space launch vehicles use oxygen:

- with jet fuel: Atlas, Thor, Jupiter, Titan I, Saturn booster;
- with hydrogen: Space Shuttle and Centaur upper stage;
- with alcohol: V-2 and Redstone.

Although it usually does not burn spontaneously with organic materials at ambient pressures, combustion or explosions can occur when a confined mixture of oxygen and organic matter is suddenly pressurized. Impact tests show that mixtures of liquid oxygen with many commercial oils or organic materials will detonate. Liquid oxygen supports and accelerates the combustion of other materials. Handling and storage are safe when contact materials are clean.

Liquid oxygen is a noncorrosive and nontoxic liquid and will not cause the deterioration of clean container walls. When in prolonged contact with human skin, the cryogenic propellant causes severe burns. Because liquid oxygen evaporates rapidly, it cannot be stored readily for any great length of time. If liquid oxygen is used in large quantities, it is often produced very close to its geographical point of application. Liquid oxygen can be obtained in several ways, such as by boiling liquid nitrogen out of liquid air. It is necessary to insulate all lines, tanks, valves, and so on, that contain liquid oxygen in order to reduce the evaporation loss. Rocket propulsion systems which remain filled with liquid oxygen for several hours and liquid oxygen storage systems have to be well insulated against absorbing heat from the surroundings. External drainage provisions have to be made on all liquid oxygen tanks and lines to eliminate the water that condenses on the walls [10].

#### 4.2.3 *In-flow mixture choice*

The fact that we have completely different condition between fuel and oxidizer tanks bring a serious problem on the choice of which kind of mixture we have to introduce in tanks avoiding any risk of explosion. The idea is to operate a dilution of the mixture to have in itself inert components that do not react with fuel and with oxidizer.

It is brought out a comparison between two different couples of propellant:

- RP<sub>1</sub>-LOX
- UDMH-NTO.

Oxidizer	Fuel	O/F	$\rho$ [kg/m <sup>3</sup> ]	$T_c$ [K]	$c^*$ [m/s]	$M_m$ [g/mol]	$t_{sp}^{sh}$ [s]	$t_{sp}^{tr}$ [s]
LOX	CH <sub>4</sub>	3.20	1.19	3526	1835			296
		3.00	1.11	3526	1853		311	
	N <sub>2</sub> H <sub>4</sub>	0.74	1.06	3285	1871	18.3		301
		0.90	1.07	3404	1892	19.3	313	
Flourine	LH <sub>2</sub>	3.40	0.21	2959	2428	8.9		386
		4.02	0.25	2999	2432	10.0	389.5	
	RP-1	2.24	1.59	3571	1774	21.9	285.4	300
	UMDH	2.56	1.82	3677	1800	23.3		295
NTO		1.39	0.96	3542	1835	19.8		
	N <sub>2</sub> H <sub>4</sub>	1.65	1.14	3594	1864	21.3	310	
		1.83	1.29	4553	2128	18.5		334
	LH <sub>2</sub>	2.30	1.54	4713	2208	19.4	365	
Aerozine		4.54	0.21	3080	2534	8.9		389
		7.60	0.35	3900	2549	11.8	410	
	N <sub>2</sub> H <sub>4</sub>	1.08	0.75	3258	1765	19.5		283
		1.34	0.93	3152	1782	20.9	292	
Red fuming nitric acid		1.62	1.01	3242	21.0			278
		2.00	1.24	3372	1652	22.6	289	
	RP-1	3.4	1.05	3290	1711	24.1	297	
	MMH	2.15	1.30	3396	1747	22.3	289	
H <sub>2</sub> O <sub>2</sub>		1.65	1.16	3200	1591	21.7		278
	RP-1	4.1	2.12	3175	1594	24.6	269	258
		4.8	2.48	3230	1609	25.8		
	Aerozine	1.73	1.00	2997	1682	20.6	279	272
	2.20	1.26	3172	1701	22.4			
	RP-1	7.0	4.01	2760	21.7			297

Table 18: Theoretical Performance of Liquid Rocket Propellant Combinations



For this propellants has been analyzed the trend of composition and temperature with the dilution ratio, with the aim to find the most suitable combination that allow the faster evaporation preventing risks of dangerous chemical reaction in tanks.

The comparison is also made at different two different choice of O/F ratio:

- RP1-LOX  $\rightarrow$  O/F = 2.34 (typical working condition)
- RP1-LOX  $\rightarrow$  O/F  $\sim$  3.3 (stoichiometric condition)
- UDMH-NTO  $\rightarrow$  O/F = 2.0 (typical working condition)
- UDMH-NTO  $\rightarrow$  O/F  $\sim$  2.9 (stoichiometric condition)

Through CEA, a software developed by NASA used to execute chemical operation, it is possible to see that the couple RP1-LOX for the typical operative condition has brought out this result, considering a combustion followed by a dilution.

Here are reported analyses for fuel tank.

These results correspond to a dilution after a combustion at 8 bar in a gas generator.

For fuel tank we obtain as follow in table 19 considering an O/F = 2.34.

$\frac{\dot{m}_{dil}}{\dot{m}_{comb}}$	1	2.5	5	10	15	20	25	30
CH4	0.05869	0.17995	0.30826	0.41407	0.45524	0.47647	0.48931	0.49789
CO	0.45046	0.10406	0.01786	0.00237	0.00076	0.00036	0.00021	0.00014
CO2	0.05542	0.05455	0.02164	0.00555	0.00234	0.00126	0.00078	0.00053
C2H4	$10^{-5}$	0	0	0	0	0	0	0
C2H6	$10^{-5}$	$2 \cdot 10^{-5}$	$2 \cdot 10^{-5}$	$4 \cdot 10^{-5}$	$4 \cdot 10^{-5}$	$4 \cdot 10^{-5}$	$4 \cdot 10^{-5}$	$3 \cdot 10^{-5}$
H2	0.06997	0.05451	0.03529	0.02025	0.01481	0.01212	0.01055	0.00953
H2O	0.05935	0.11381	0.10228	0.06565	0.04690	0.03630	0.02957	0.02492
C(gr)	0.30611	0.49309	0.51464	0.49206	0.47991	0.47344	0.46954	0.46696
T [K]	1156	1001	893	803	763	739	724	712

Table 19: Mass flow composition into tank for RP1-LOX at O/F = 2.34

The results in which the combustion inside at gas generator is made at stoichiometric condition is the following reported in table 20.

Considering the hipergolic couple UDMH-NTO, for fuel tank, the composition of the mass flow injected into the tank is shown in table ??, for an O/F = 2.

Assuming a stoichiometric O/F ratio (O/F=2.9) for UDMH-NTO regarding the combustion inside the gas generator, we obtain the following conditions at the exhaust of gas generator reported in table 22

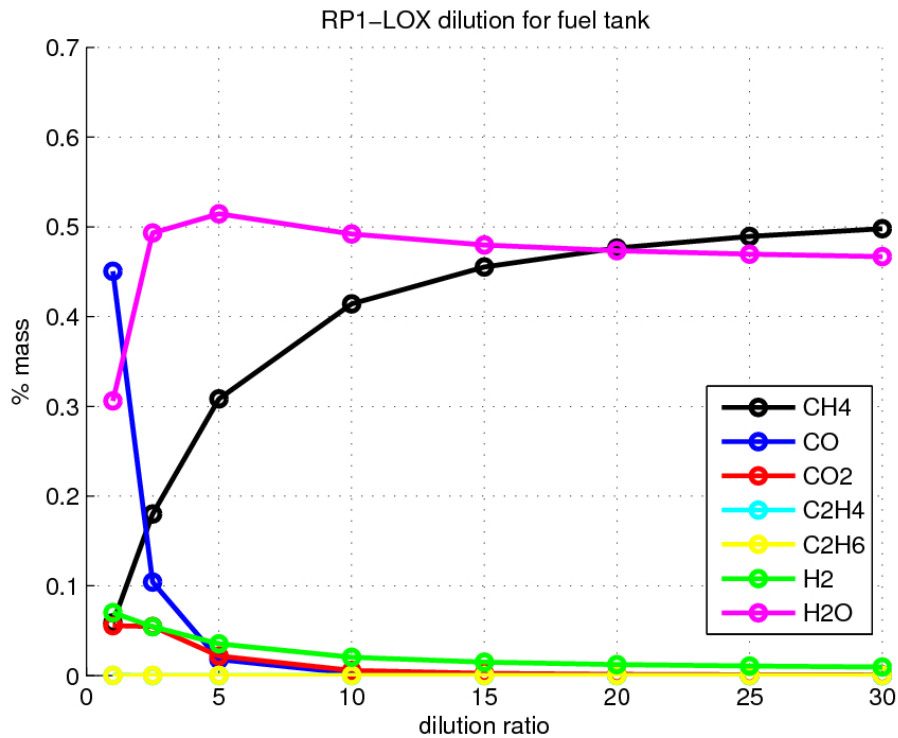


Figure 32: Mass flow into the tank for RP1-LOX at O/F = 2.34

From the results obtained it is possible to understand that the choice of hypergolic couple is not properly suitable for the design indications. In fact the temperature have to be less than 900 K, so this choice is to be avoided due to the high temperature of the gases. RP1-LOX combination shows a well suitable conditions of the exhaust from gas generator to the aim of gasification. In fact we have temperatures low enough to be introduced in fuel tank, composition that does not react with the element present in tank, and it is also evident that the dilution ratio is not extremely high to obtain the exhaust condition required, in this way the amount of mass that have to be equipped for the de-orbiting maneuver tends to be limited.

The results show also the fact that the composition coming out from hypergolic couple contain compounds that could react with the elements contained into the tank. So, for the fuel tank, the most suited choice corresponds in the RP1-LOX couple, at an O/F ratio of 2.34, the typical working O/F, and choosing a dilution ratio greater than 5.

Now we consider the oxidizer tank and the choice for the most suitable mixture to be introduced which does not produce dangerous chemical reactions inside the tank.

$\frac{\dot{m}_{dil}}{\dot{m}_{comb}}$	1	2.5	5	10	15	20	25	30
CH <sub>4</sub>	0.04288	0.15802	0.28797	0.40149	0.44664	0.47003	0.48419	0.49365
CO	0.54654	0.13629	0.02435	0.00318	0.00100	0.00046	0.00026	0.00017
CO <sub>2</sub>	0.04423	0.05995	0.02609	0.00685	0.00289	0.00155	0.00096	0.00065
C <sub>2</sub> H <sub>4</sub>	$10^{-5}$	$2 \cdot 10^{-5}$	$2 \cdot 10^{-5}$	$4 \cdot 10^{-5}$	$4 \cdot 10^{-5}$	$4 \cdot 10^{-5}$	$4 \cdot 10^{-5}$	$3 \cdot 10^{-5}$
H <sub>2</sub>	0.07093	0.05775	0.03829	0.02197	0.01592	0.01293	0.01117	0.01003
H <sub>2</sub> O	0.04434	0.11016	0.10700	0.07091	0.05101	0.03958	0.03228	0.02724
C(gr)	0.25107	0.47780	0.51626	0.49556	0.48251	0.47541	0.47109	0.46823
T [K]	1195	1021	909	815	772	747	730	719

Table 20: Mass flow composition into tank for RP<sub>1</sub>-LOX at O/F = 3.3

$\frac{\dot{m}_{dil}}{\dot{m}_{comb}}$	1	2.5	5	10	15	20	25	30
CH <sub>4</sub>	0.02649	0.08172	0.13148	0.17343	0.19170	0.20187	0.20835	0.21284
CO	0.37926	0.17619	0.08354	0.037886	0.02396	0.01742	0.01365	0.01121
CO <sub>2</sub>	0.00596	0.00901	0.00537	0.00212	0.00110	0.00067	0.00045	0.00032
C <sub>2</sub> H <sub>4</sub>	$10^{-5}$	$10^{-5}$	0	0	0	0	0	0
C <sub>2</sub> H <sub>6</sub>	0	$10^{-5}$	$2 \cdot 10^{-5}$	$2 \cdot 10^{-5}$	$3 \cdot 10^{-5}$	$3 \cdot 10^{-5}$	$3 \cdot 10^{-5}$	$3 \cdot 10^{-5}$
HCN	$14 \cdot 10^{-5}$	$3 \cdot 10^{-5}$	$2 \cdot 10^{-5}$	$2 \cdot 10^{-5}$	$3 \cdot 10^{-5}$	$3 \cdot 10^{-5}$	$3 \cdot 10^{-5}$	$3 \cdot 10^{-5}$
H <sub>2</sub>	0.08137	0.08479	0.08285	0.07991	0.07841	0.07754	0.07697	0.07657
H <sub>2</sub> O	0.01225	0.02849	0.02890	0.02136	0.01632	0.01311	0.01094	0.00937
NH <sub>3</sub>	0.00025	0.00053	0.00072	0.00086	0.00092	0.00095	0.00096	0.00098
N <sub>2</sub>	0.41195	0.43488	0.44756	0.45561	0.45863	0.46021	0.46118	0.46184
C(gr)	0.08231	0.18435	0.21954	0.22879	0.22892	0.22819	0.22746	0.22684
T [K]	1280	1140	1082	1046	1032	1025	1021	1018

Table 21: Mass flow composition into tank for UDMH-NTO at O/F = 2

Also in this case the comparison is brought out considering the storable couple UDMH-NTO, and the couple of propellant used by Block I itself, i.e. RP<sub>1</sub>-LOX.

In the table 23 is reported the analysis for the estimation of the mass flow composition going inside the oxidizer tank for RP<sub>1</sub>-LOX at O/F=2.34.

Results for analysis for the stoichiometric condition about RP<sub>1</sub>-LOX are given in table 24 and in fig. 37.

Considering UDMH-NTO propellant couple CEA analyses produced results reported in table 25 and figure 38.

For stoichiometric combustion of UDMH-NTO it has been obtained the following results presented in table 26 and figure 39.

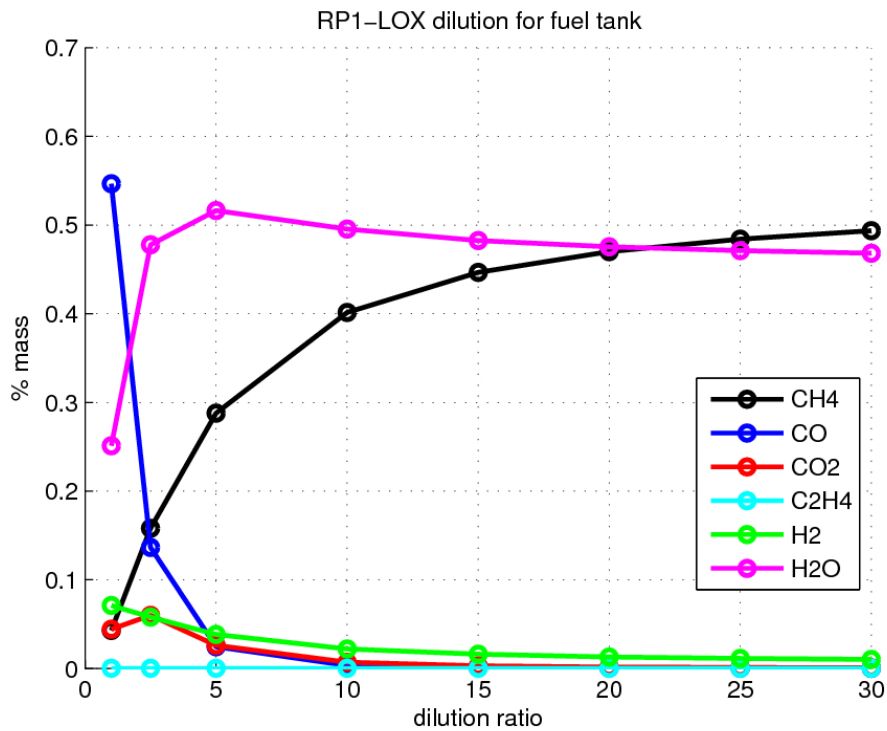


Figure 33: Mass flow into the tank for RP1-LOX at O/F = 3.3

About dilution for oxidizer tank we need just to consider which dilution ratio choose, due to the fact that the choice about the propellant couple has been made considering the performances for the dilution of fuel tank.

Considering the fact that RP1-LOX, working at O/F = 2.34, is the most suitable choice, the dilution ratio, that must be taken to fit the request, should be greater than 10, approximatively around 15 (that will be the final choice).

In the end it has been obtained the following choices:

- additional propellant: RP1-LOX
- fuel dilution ratio:5
- oxidizer dilution ratio 15

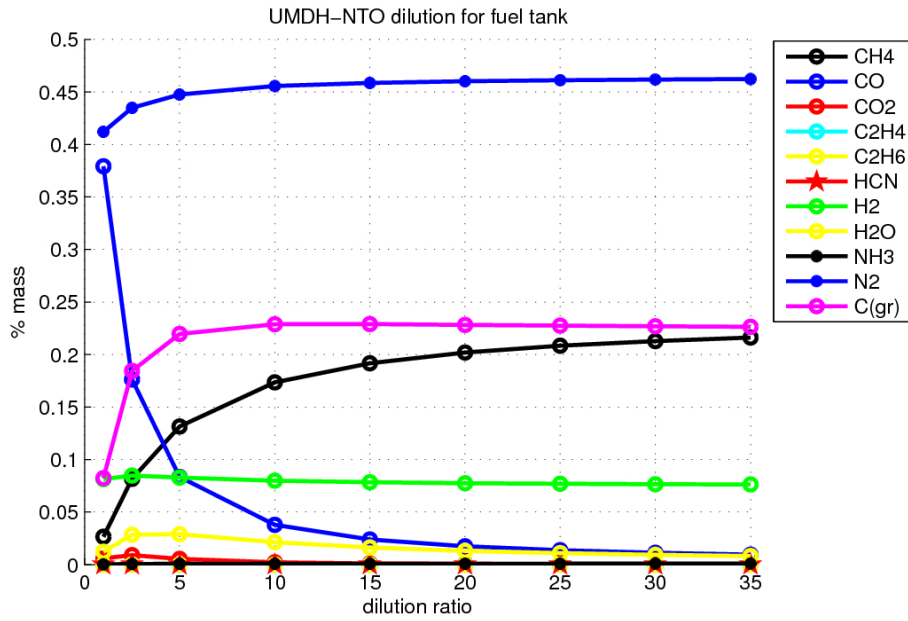


Figure 34: Mass flow into the tank for UDMH-NTO at O/F = 2

$\frac{\dot{m}_{dil}}{\dot{m}_{comb}}$	1	2.5	5	10	15	20	25	30
CH4	0.01753	0.07072	0.12224	0.16706	0.18692	0.19807	0.20519	0.21014
CO	0.43506	0.20531	0.09693	0.04348	0.02732	0.01977	0.01545	0.01266
CO2	0.00407	0.00933	0.00616	0.00255	0.00134	0.00082	0.00055	0.00039
C2H4	10 <sup>-5</sup>	10 <sup>-5</sup>	0	0	0	0	0	0
C2H6	0	10 <sup>-5</sup>	2 · 10 <sup>-5</sup>	2 · 10 <sup>-5</sup>	3 · 10 <sup>-5</sup>	3 · 10 <sup>-5</sup>	3 · 10 <sup>-5</sup>	3 · 10 <sup>-5</sup>
HCN	22 · 10 <sup>-5</sup>	4 · 10 <sup>-5</sup>	2 · 10 <sup>-5</sup>	10 <sup>-5</sup>	10 <sup>-5</sup>	10 <sup>-5</sup>	10 <sup>-5</sup>	10 <sup>-5</sup>
H2	0.07894	0.08482	0.08338	0.08040	0.07881	0.07787	0.07725	0.07681
H2O	0.00803	0.02670	0.02968	0.02289	0.01773	0.01434	0.01201	0.01032
NH3	0.00019	0.00048	0.00069	0.00084	0.00090	0.00093	0.00095	0.00097
N2	0.40574	0.43136	0.44551	0.45450	0.45787	0.45963	0.46071	0.46145
C(gr)	0.05019	0.17122	0.21538	0.22825	0.22908	0.22853	0.22784	0.22722
T [K]	1336	1157	1091	1051	1036	1028	1023	1020

Table 22: Mass flow composition into tank for UDMH-NTO at O/F = 2.9

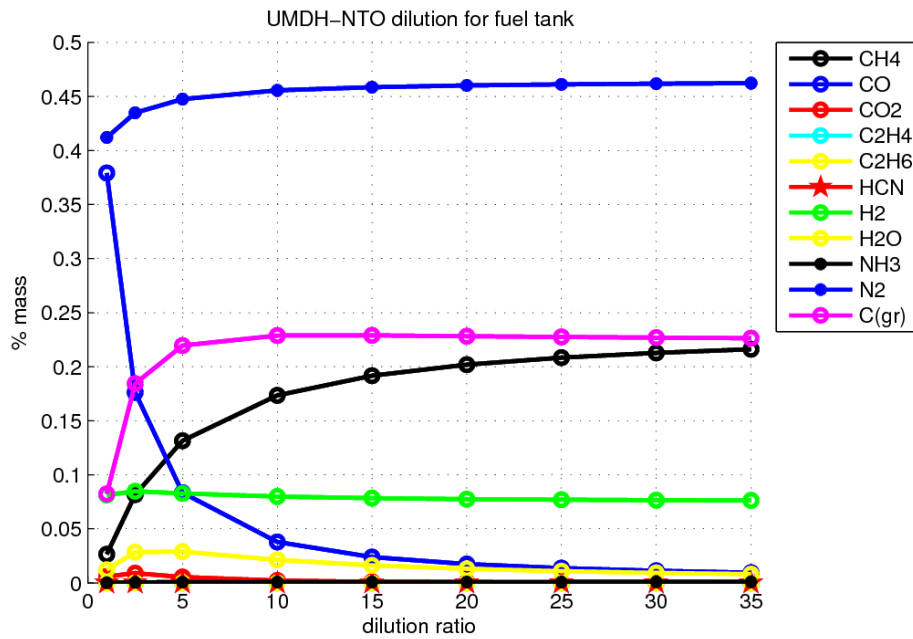


Figure 35: Mass flow into the tank for UDMH-NTO at O/F = 2.9

$\frac{\dot{m}_{dil}}{\dot{m}_{comb}}$	1	2.5	5	10	15	20	25	30
CO	0.08175	0.00560	0.00001	0	0	0	0	0
CO <sub>2</sub>	0.34295	0.26056	0.15712	0.08571	0.05892	0.04489	0.03626	0.03041
H	0.00035	0.00002	0	0	0	0	0	0
HO <sub>2</sub>	0.00024	0.00011	0.00001	0	0	0	0	0
H <sub>2</sub>	0.00082	0.00006	0	0	0	0	0	0
H <sub>2</sub> O	0.15155	0.09976	0.06250	0.03420	0.02351	0.01791	0.01447	0.00887
H <sub>2</sub> O <sub>2</sub>	0.00001	0	0	0	0	0	0	0
O	0.02175	0.00391	0.00002	0	0	0	0	0
OH	0.04915	0.01331	0.00038	0	0	0	0	0
O <sub>2</sub>	0.35144	0.61667	0.77997	0.88009	0.91756	0.93719	0.94927	0.95745
H <sub>2</sub> O(L)	0	0	0	0	0	0	0	0.00327
T [K]	3168	2639	1804	1038	709	523	401	323

Table 23: Mass flow composition into oxidizer tank for RP1-LOX at O/F = 2.34

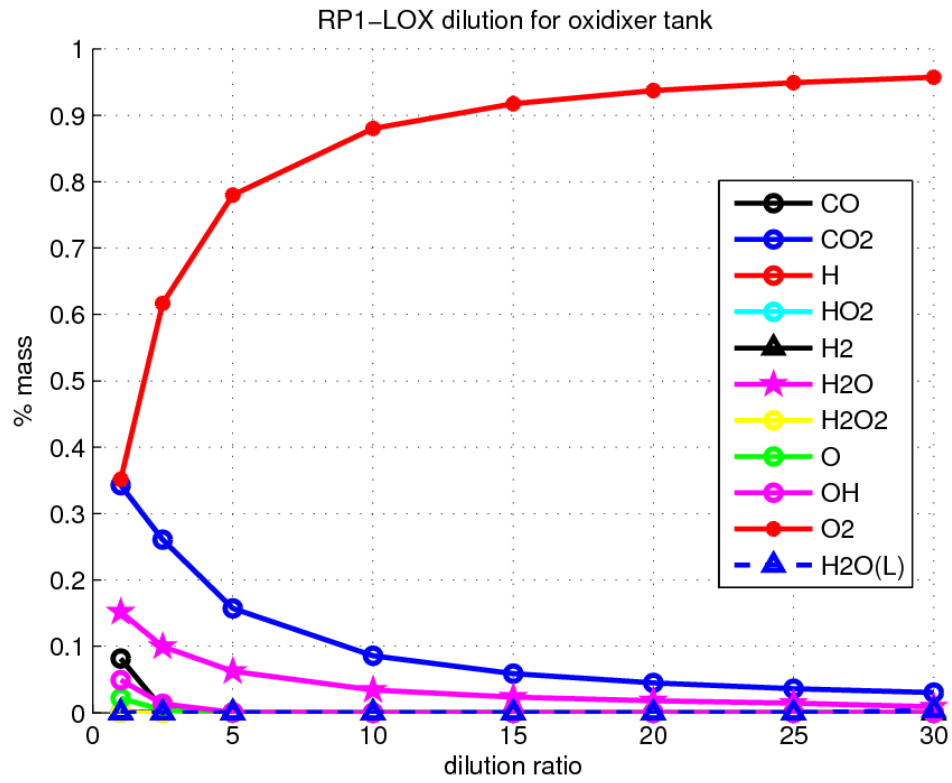


Figure 36: Mass flow into the oxidizer tank for RP1-LOX at O/F = 2.34

$\frac{\dot{m}_{dil}}{\dot{m}_{comb}}$	1	2.5	5	10	15	20	25	30
CO	0.03206	0.00052	0	0	0	0	0	0
CO2	0.31577	0.20842	0.12205	0.06657	0.04577	0.03487	0.02817	0.02362
H	0.00012	0	0	0	0	0	0	0
HO2	0.00020	0.00004	0	0	0	0	0	0
H2	0.00030	0.00001	0	0	0	0	0	0
H2O	0.12525	0.08148	0.04870	0.02657	0.01827	0.01392	0.00300	0.00002
H2O2	0.00001	0	0	0	0	0	0	0
O	0.01318	0.00060	0	0	0	0	0	0
OH	0.03221	0.00368	0.00002	0	0	0	0	0
O2	0.48090	0.70526	0.82923	0.90686	0.93596	0.95121	0.96059	0.96695
H2O(L)	0	0	0	0	0	0	0.00825	0
H2O(cr)	0	0	0	0	0	0	0	0.00940
T [K]	2975	2263	1445	806	535	381	303	242

Table 24: Mass flow composition into oxidizer tank for RP1-LOX at O/F = 3.3

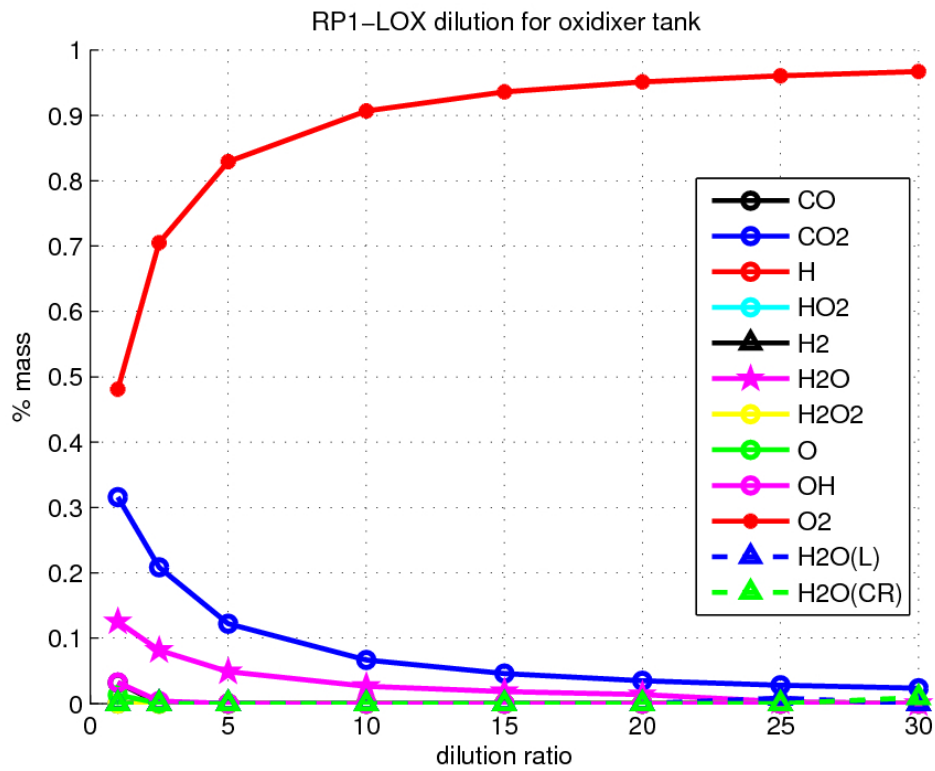


Figure 37: Mass flow into the oxidizer tank for RP1-LOX at O/F = 3.3

$\frac{\dot{m}_{dil}}{\dot{m}_{comb}}$	1	2.5	5	10	15	20	25	30
CO	0.02815	0.00052	0	0	0	0	0	0
CO <sub>2</sub>	0.19986	0.13867	0.08136	0.04438	0.03051	0.02325	0.01878	0.01575
H	0.00015	0	0	0	0	0	0	0
HO <sub>2</sub>	0.00011	0.00003	0	0	0	0	0	0
H <sub>2</sub>	0.00060	0.00001	0	0	0	0	0	0
H <sub>2</sub> O	0.17743	0.11188	0.06658	0.03634	0.02498	0.01903	0.01537	0.01289
H <sub>2</sub> O <sub>2</sub>	0.000010	0	0	0	0	0	0	0
NO	0.02816	0.01343	0.00163	0.00002	0	0	0	0
NO <sub>2</sub>	0.00007	0.00009	0.00005	0.00001	0	0	0	0
N <sub>2</sub>	0.31823	0.31355	0.31266	0.30934	0.30782	0.30702	0.30653	0.30620
O	0.00804	0.00053	0	0	0	0	0	0
OH	0.02947	0.00412	0.00007	0	0	0	0	0
O <sub>2</sub>	0.20970	0.41715	0.53764	0.60990	0.63668	0.65069	0.65932	0.66516
T [K]	2938	2280	1558	972	724	585	496	435

Table 25: Mass flow composition into oxidizer tank for UDMH-NTO at O/F = 2



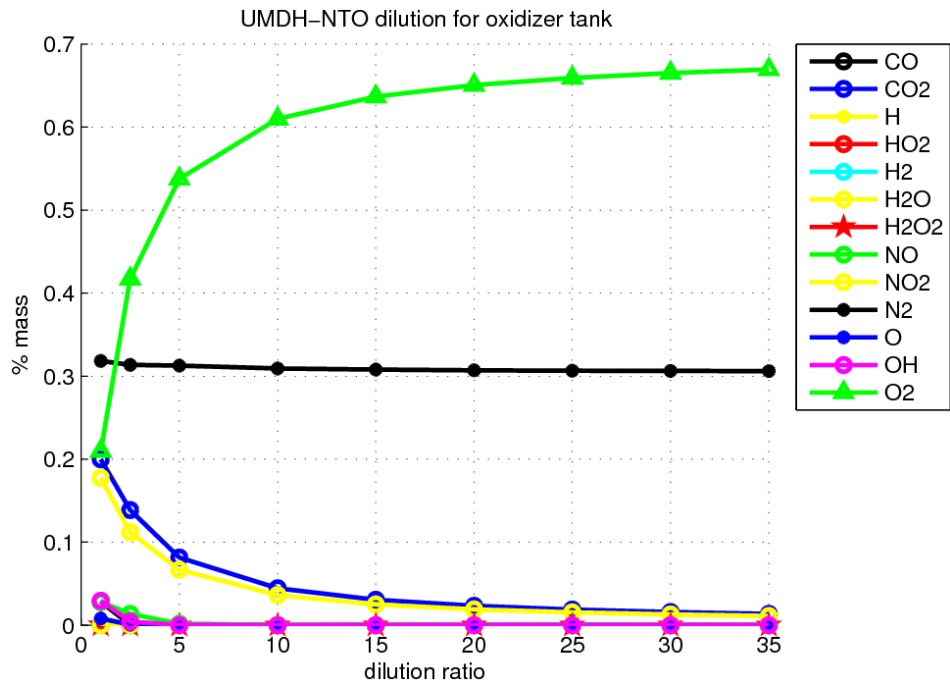


Figure 38: Mass flow into the oxidizer tank for UDMH-NTO at O/F = 2

$\frac{\dot{m}_{dil}}{\dot{m}_{comb}}$	1	2.5	5	10	15	20	25	30
CO	0.00652	0.00002	0	0	0	0	0	0
CO <sub>2</sub>	0.17751	0.10726	0.06259	0.03414	0.02347	0.01788	0.01444	0.01211
H	0.00003	0	0	0	0	0	0	0
HO <sub>2</sub>	0.00008	0.00001	0	0	0	0	0	0
H <sub>2</sub>	0.00014	0	0	0	0	0	0	0
H <sub>2</sub> O	0.14418	0.08745	0.05124	0.02795	0.01922	0.01464	0.01183	0.00992
NO	0.02365	0.00572	0.00035	0	0	0	0	0
NO <sub>2</sub>	0.00009	0.00007	0.00003	0	0	0	0	0
N <sub>2</sub>	0.31411	0.31361	0.31120	0.30822	0.30705	0.30643	0.30605	0.30579
O	0.00338	0.00004	0	0	0	0	0	0
OH	0.01514	0.00074	0	0	0	0	0	0
O <sub>2</sub>	0.31514	0.48508	0.57460	0.62968	0.65026	0.66105	0.66768	0.67217
T [K]	2672	1912	1273	791	590	478	407	359

Table 26: Mass flow composition into oxidizer tank for UDMH-NTO at O/F = 2.9

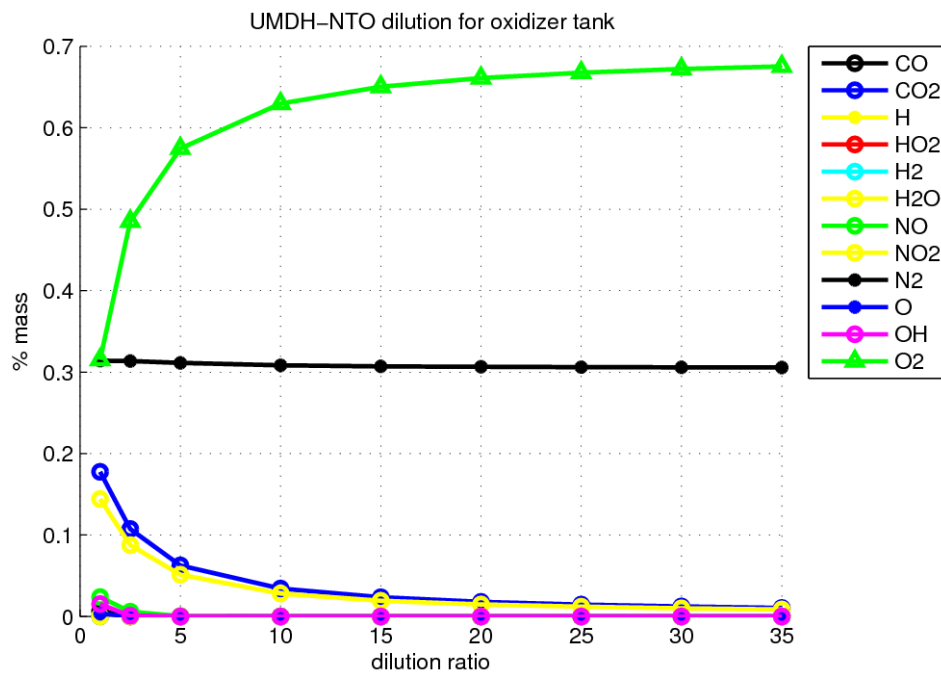


Figure 39: Mass flow into the oxidizer tank for UDMH-NTO at O/F = 2.9

## ANALYTIC MODEL

Since that the attitude conditions of Block I are unknown after the release of the upper stage, we do not know accelerations and eventual rotation velocity of the object, in this way it is difficult to know and understand the condition inside the tanks. Problems to determine how the liquid is disposed into tanks are several and difficult to solve, so it is necessary to introduce some hypothesis which allow an easier solution of the task. As said problems are several, the main are the condition of liquid inside the tanks, how it is disposed, where exactly is placed, presence of liquid bubble, impossibility to determine the velocity of the liquid and its convective motion, effect of low gravity and the estimation of the real acceleration which affect the Block I.

The first hypothesis is to suppose no presence of bubbles, so the liquid is all collected in one single volume, on the second we assume that this liquid is disposed on the bottom of the tank, in this way we consider the worst condition for heat exchange because we consider the lowest area possible for convection heat exchange between gas and liquid.

Due to the lack of the attitude conditions, we report two different way to evaluate temperature inside the liquid. The first way is based on a zero-dimensional model in which we consider natural convection inside the the liquid, the second is a one-dimensional model in which we assume the liquid motionless, so there is only the presence of thermal diffusion.

## 5.1 CONVECTION-BASED MODEL

In this zero-dimensional model we consider to evaluate liquid temperature basing on natural convection inside liquid, instead warm gases exchange heat with liquid by forced convection. In table are present typical value for natural and forced convection [3].

<b>Free convection</b>	
Gases	2 – 25
Liquids	50 – 1000
<b>Forced convection</b>	
Gases	25 – 250
Liquids	100 – 20,000

Table 27: Typical coefficient for heat transfer convection [3]

By energy balance we estimate the gas temperature,  $T_{gas}$  at each instant:

$$M_{gas}c_{pgas}T_{gas} + \dot{m}_{in}c_{pin}T_{in}dt + \dot{m}_{ev}c_{pev}T_{ev}dt - \dot{m}_{out}c_{pout}T_{out}dt = 0 \quad (5.1)$$

where  $M_{gas}$  is the gas mass contained in tank at each instant,  $c_{pgas}$ , the specific heat,  $\dot{m}_{in}$  the mass flow coming into tank from gas generator,  $c_{pin}$  the specific heat of the mass flow and  $T_{in}$  its temperature,  $\dot{m}_{ev}$  the mass flow related to the evaporation process,  $c_{pev}$  and  $T_{ev}$  is the corresponding specific heat and temperature, instead  $\dot{m}_{out}, c_{pout}, T_{out}$  are the mass flow, specific heat and temperature of the eventual mass flow going outside of the tank,  $dt$  is the time-step. Proceeding in this way we overlook and the eventual possibility of a flow rate due to the condensation of gases [11].

Once obtained  $T_{gas}$ , seen that we consider a zero-dimensional model for gas phase, it is possible to evaluate the heat transfer from gas to liquid.

$$M_{liq}c_{liq}\frac{\partial T_{liq}}{\partial t} = q_{net} \quad (5.2)$$

where:

$$q_{net} = q_{in} - q_{ev} + q_{out}$$

$$q_{in} = hA(T_{gas} - T_{int})$$

$$q_{ev} = \dot{m}_{ev}c_{pev}T_{ev}$$

$$q_{liq} = h_{liq}A(T_{int} - T_{liq})$$

whence,  $A$  is the area of exchange,  $h$  the transfer heat coefficient between gas and liquid,  $h_{liq}$  is the transfer heat coefficient for natural convection,  $T_{int}$  that coincide with  $T_{ev}$  is the temperature of the interface between liquid and gas.

Evaluated  $T_{liq}$  we calculate the evaporation rate through the Hertz-Kundsen-Langmuir 5.3 equation [12] [13]:

$$\dot{m}_{net} = \sqrt{\frac{M_m}{2\pi R_u}} \cdot \left( \sigma_{ev} \frac{P_{vp}}{\sqrt{T_{liq}}} - \sigma_c \frac{P_{gas}}{\sqrt{T_{gas}}} \right) \quad (5.3)$$

where  $\dot{m}_{net}$  is the net mass flow between evaporation and condensation,  $\sigma_{ev}$  and  $\sigma_c$  are experimental constant ( $0 < \sigma_{ev}, \sigma_c < 1$ ) (in this case  $\sigma_c = 0$ ),  $P_{vp}$  is the vapor pressure,  $M_m$  is the molar mass and  $R_u$  is the universal constant for gases.

The algorithm works in this way: given a  $T_{int}$  of guess, it proceeds with the evaluation of  $T_{gas}, T_{liq}$  and  $\dot{m}_{ev}$ , then it is made an energy balance at interface:

$$\Delta q = q_{in} - q_{ev} - q_{out}$$

in order to obtain the correct  $T_{\text{int}}$ . The iteration goes on till  $\Delta q = 0$ .

Once estimated the correct  $T_{\text{int}}$  we can calculate the correct  $T_{\text{gas}}$ ,  $T_{\text{liq}}$ ,  $\dot{m}_{\text{ev}}$ . Now is possible to update the moles of gases, in order to calculate  $c_{p_{\text{gas}}}$ ,  $M_{m_{\text{gas}}}$  and all the other quantities.

Seen that we consider the combining mixing rules for mixture proposed by Van der Waal 5.4 [1] [14], every property of the gas mixture must be estimated as follows.

$$Q_m = \sum_i \sum_j y_i y_j Q_{ij} \quad (5.4)$$

$$Q_{ij} = \frac{k_{ij} (Q_{ii} + Q_{jj})}{2}$$

$$k_{ij} = \frac{8 (V_{c_i} \cdot V_{c_j})^{1/2}}{(V_{c_i}^{1/3} + V_{c_j}^{1/3})^3}$$

where  $V_c$  is the critical volume and  $Q_{ii} = Q_i$ .

Once known  $\dot{m}_{\text{ev}}$  are known also the left liquid mass, and the volume occupied by gas, so even the density  $\rho$  of the mixture is known.

To evaluate the pressure we consider the law for real gases, in which it is introduced the compressibility factor  $Z$  5.5 [1] [14].

$$PV = ZRT \quad (5.5)$$

$Z$  is obtained by the virial equation 5.6 [1] [14]

$$Z = 1 + \frac{BP}{RT} \quad (5.6)$$

where  $B$  [1] [14] is defined as

$$B = \lim_{1/V \rightarrow 0} \left( \frac{\partial Z}{\partial 1/V} \right)_T$$

but it is common calculated as

$$\frac{P_c B}{RT_c} = B^{(0)} + \omega B^{(1)}$$

$$B^{(0)} = 0.083 - \frac{0.422^{1.6}}{T_r}$$

$$B^{(1)} = 0.139 - \frac{0.172^{4.2}}{T_r}$$

where  $T_r = T/T_c$  is the reduced temperature, instead  $\omega$  5.7 is the acentric factor [15] and it is defined as:

$$\omega = -\text{Log} P_{\text{vpr}} (\text{at } T_r = 0.7) - 1 \quad (5.7)$$

but it is calculated through

$$\omega = \frac{3}{7} \frac{T/T_r}{1 - T/T_r} \text{Log} P_c - 1$$

Liquid density trend with temperature has been obtained through Rackett correlation [1] [14] in 5.8

$$V_s = \frac{RT_c}{P_c} Z_{RA}^{[1+(1-T_r)^{2/7}]} \quad (5.8)$$

$$Z_{RA} = 0.29056 - 0.08775\omega$$

The heat capacity for a real gas can be evaluated as follow:

$$C_p = C_p^o + \Delta C_p \quad (5.9)$$

$$\Delta C_p = T \int_{\infty}^V \left( \frac{\partial^2 P}{\partial T^2} \right) dV - \frac{T (\partial P / \partial T)_V^2}{(\partial P / \partial V)_T} - R$$

For the Lee-Kesler method 5.10  $C_p$  [1] [14] is given by:

$$C_p + C_p^o = \Delta C_p = (\Delta C_p)^{(o)} + \omega(\Delta C_p)^{(1)} \quad (5.10)$$

where  $\Delta C_p^{(o)}$  and  $\Delta C_p^{(1)}$  are value tabled in function of  $T_r$  and  $P_r$ .

Another Lee-Kesler [1] [14] correlation is used to evaluate the trend of heat capacity with temperature for liquid in eq.5.11

$$\frac{C_{pL} - C_p^o}{R} = 1.45 + .45(1 - T_r)^{-1} + .25\omega(17.11 + 25.2(1 - T_r)^{(1/3)}(T_r)^{-1} + 1.742(1 - T_r)^{-1}) \quad (5.11)$$

Vapor pressure of RP-1 with temperature trends has been estimated by Lee-Kesler method [1] [14], instead for LOX the value are table in an article form NASA [16], however the correlation for fuel is:

$$\ln P_{vp_r} = f^{(0)} + \omega f^{(1)} \quad (5.12)$$

$$f^{(0)} = 5.92714 - 6.09648/(T_r) - 1.28862 \text{Log}(T_r) + .169347(T_r)^6$$

$$f^{(1)} = 15.2518 - 15.6875/(T_r) - 13.4721 \text{Log}(T_r) + .43577(T_r)^6$$

Instead trend of kinetic viscosity for liquid with temperature [1] [14] is:

$$\mu_L^{-0.2661} = \mu_K^{-0.2661} + \frac{T - T_k}{233} \quad (5.13)$$

and thermal conductivity [1] [14] trend is given by

$$\kappa = \frac{A(1 - T_r)^{.38}}{(T_r)^{(1/6)}} \quad (5.14)$$

where

$$A = \frac{A^* T_c^\alpha}{W^\beta T_b^\gamma}$$

The heat transfer correlation in equation 5.15 [17] used is:

$$Nu = 0.58(GrPr)^{.2} \quad (5.15)$$

as already said the attitude condition are unknown, so we do not know exactly which acceleration affect the system, so in figure 40 is reported an estimated trend for  $h$  versus gravity ratio. For sure the correlation will not be correct when ratio is too high, but for low ratio ( $\sim 1$ ), it could be considered quite correct.

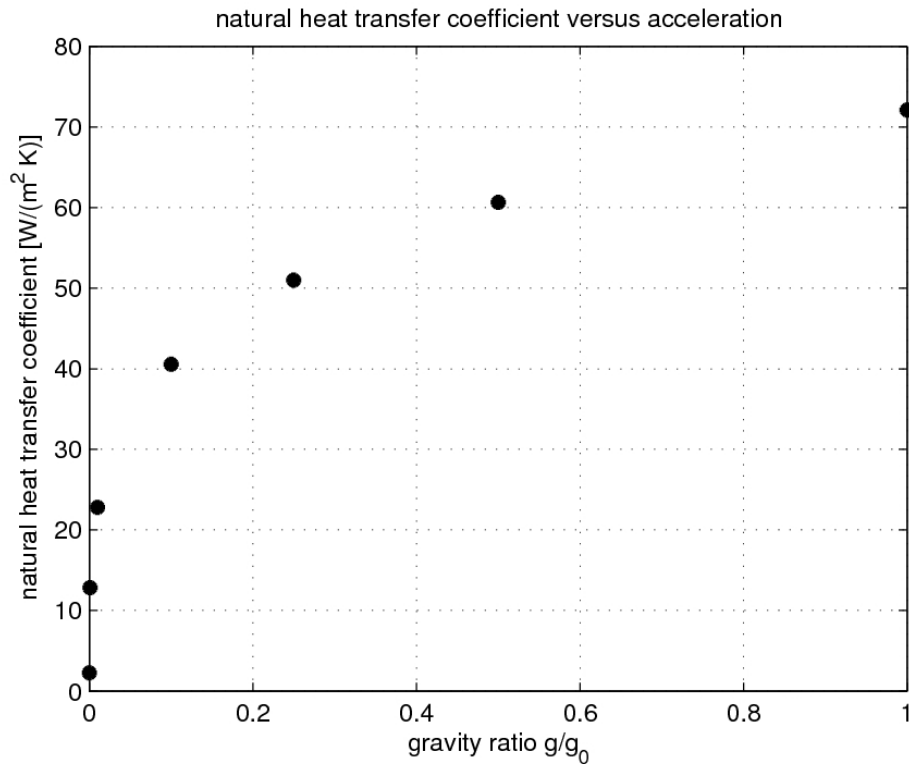


Figure 40:  $h$  versus acceleration ratio

## 5.2 DIFFUSION-BASED MODEL

In this case we consider an heterogeneous model in which the gas fraction is considered zero-dimensional, instead the liquid fraction is a one dimensional system. As said in this case liquid is motionless and the only way to transfer heat inside of itself is by diffusion, so the temperature field in liquid will be obtained by integration of the equation of diffusion.

The steps is the same as the steps presented for the case of convection transfer, but now the temperature inside the liquid must be estimated through:

$$\frac{\partial T}{\partial t} = \alpha \frac{\partial^2 T}{\partial x^2} \quad (5.16)$$

The algorithm to obtain correct temperature field for liquid and gas phases must iterate on  $\Delta q$ , that in this case is:

$$\Delta q = q_{in} - q_{ev} - q_{out}$$

$$q_{in} = hA (T_{gas} - T_{int})$$

$$q_{ev} = \dot{m}_{ev} c_{p_{ev}} T_{ev}$$

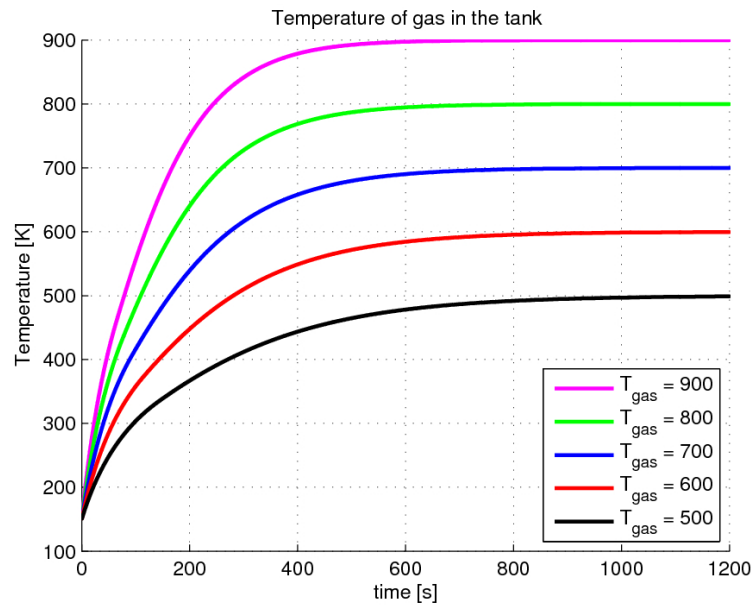
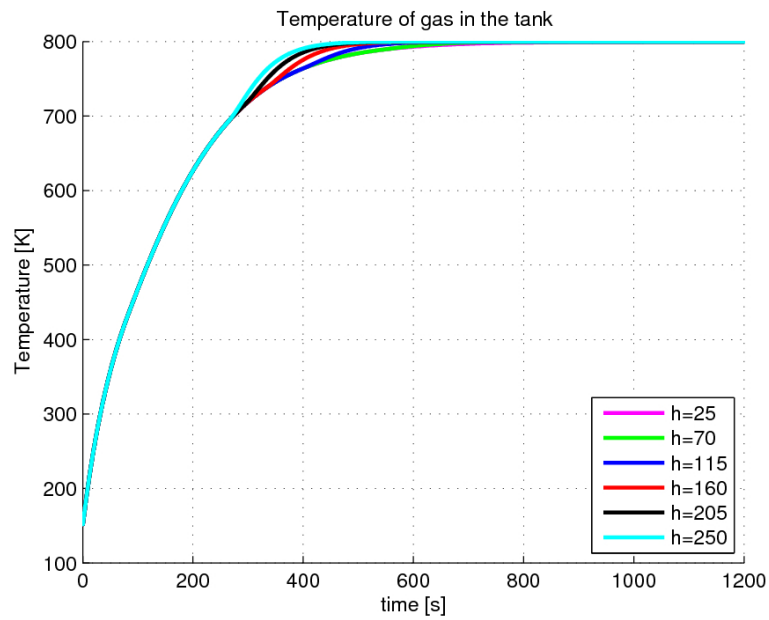
$$q_{liq} = -\kappa \left. \frac{\partial T}{\partial x} \right|_{T_{int}}$$

## 5.3 RESULTS

Here are reported some parametric results of the analysis useful to understand better which are the better working condition of the system. The parameter considered are the temperature of gases coming out from gas generator, the forced heat transfer coefficient and the amount of mass flow injected.

From parametric analysis the best choice seem to be choosing a  $T_{in}$  of 800 K, and a mass flow  $\dot{m}_{in}$  of 0.1 kg/s for fuel tank. This choice comes from a compromise between a faster evaporation and a corresponding weight of the gasification system, that should be the lowest possible in order not to create problems on the payload capability of the rocket. For oxidizer tank the considerations must be different because LOX is kept at a temperature of 90 K, but it evaporates at 92 K, this fact concern the serious and dangerous problem of the flash evaporation. In fact since LOX reach a temperature of 92 K, it immediately evaporates, producing an explosion of oxidizer tank, thus generating other space debris, so the choice must be kept considering the problem of flash evaporation. In this way it has been chosen a  $T_{in}$  of 700 K and a very small mass flow



Figure 41:  $T_{\text{gas}}$  versus  $T_{\text{in}}$  fuel tankFigure 42:  $T_{\text{gas}}$  versus  $h$  fuel tank

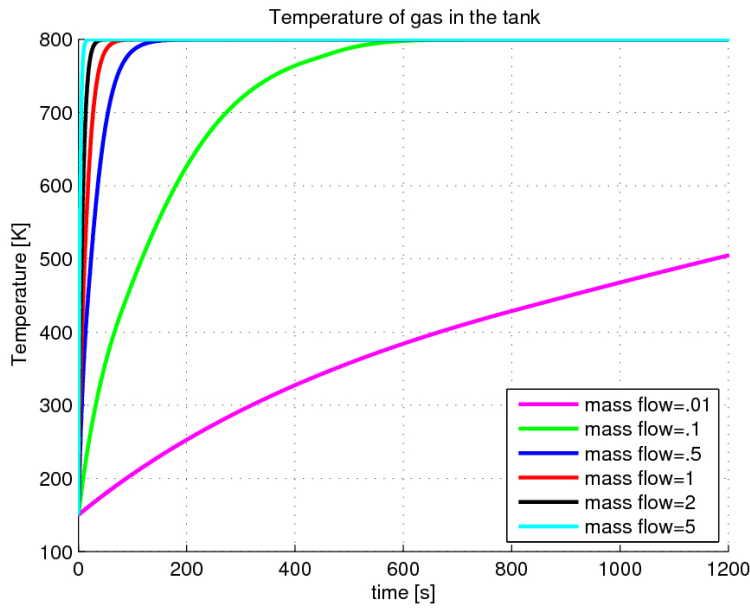


Figure 43:  $T_{gas}$  versus  $\dot{m}_{in}$  fuel tank

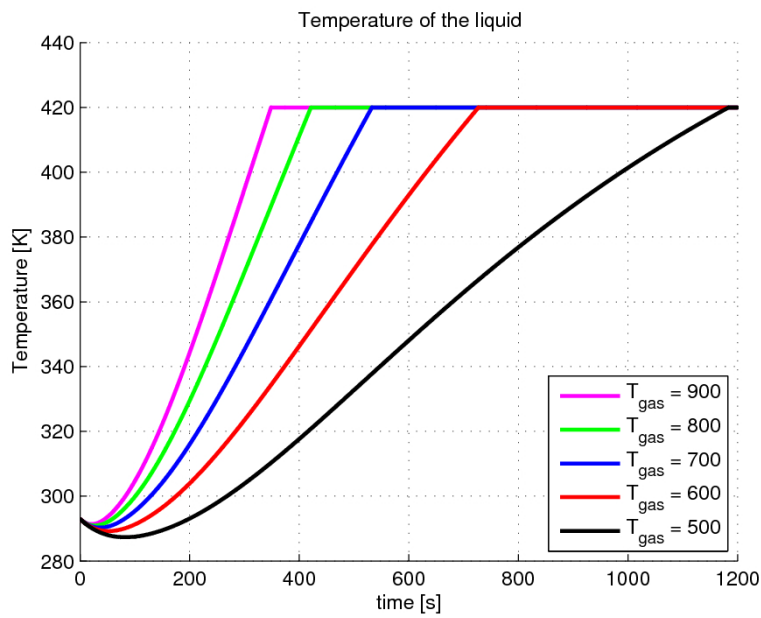
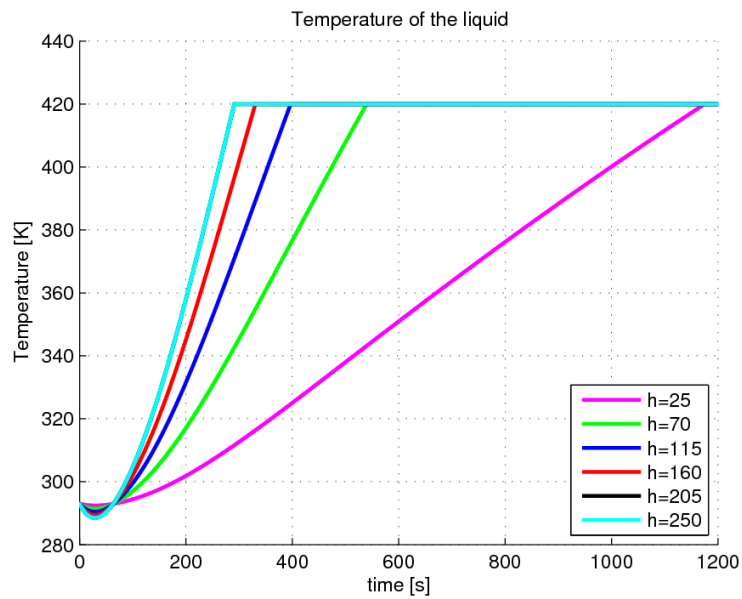
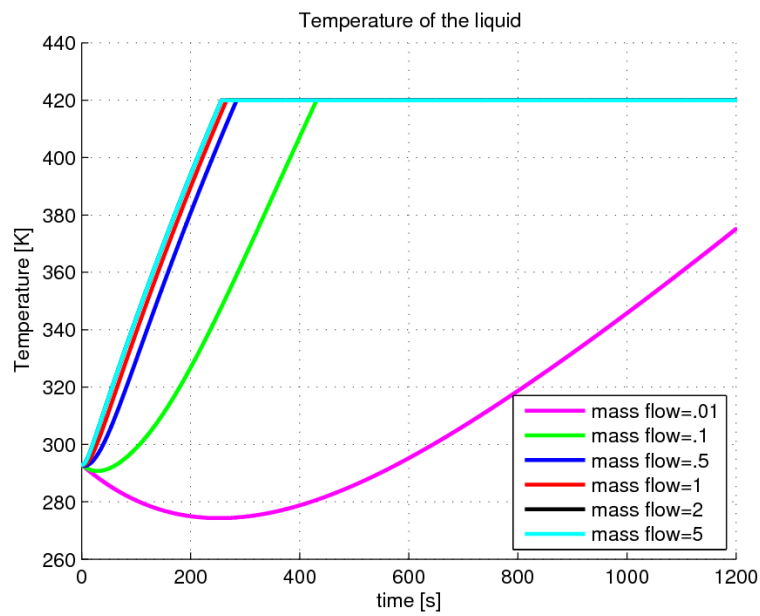


Figure 44:  $T_{liq}$  versus  $T_{in}$  fuel tank

Figure 45:  $T_{liq}$  versus  $h$  fuel tankFigure 46:  $T_{liq}$  versus  $\dot{m}_{in}$  fuel tank

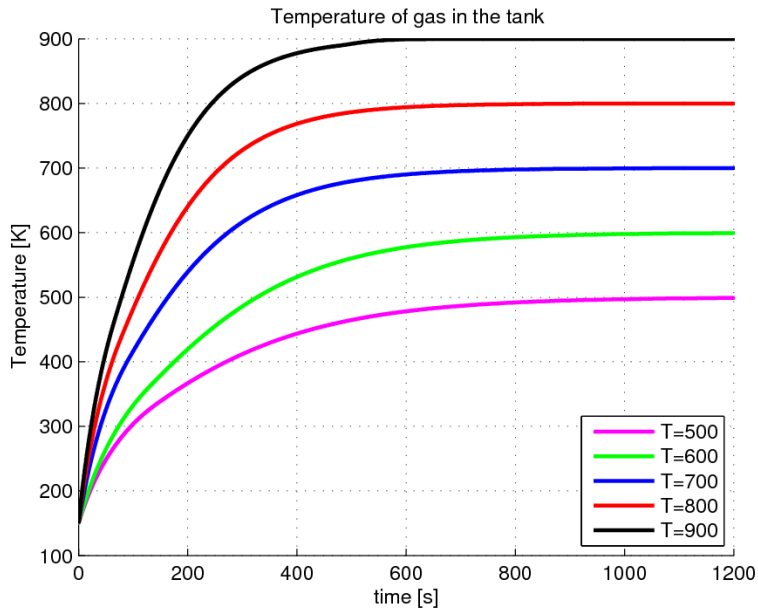


Figure 47:  $T_{gas}$  versus  $T_{in}$  fuel tank diffusive model

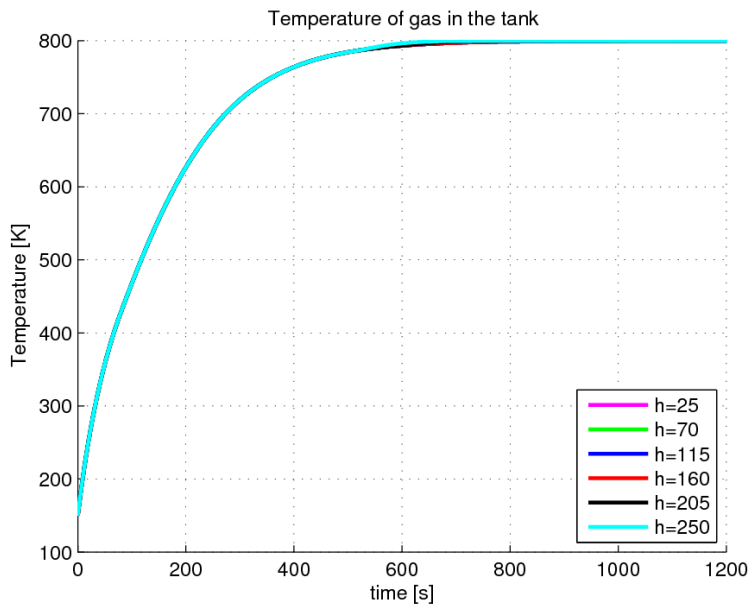
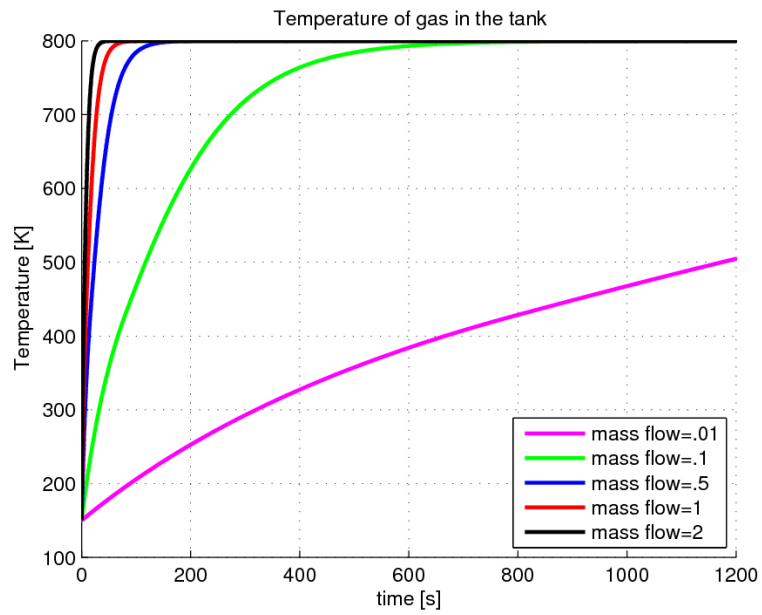
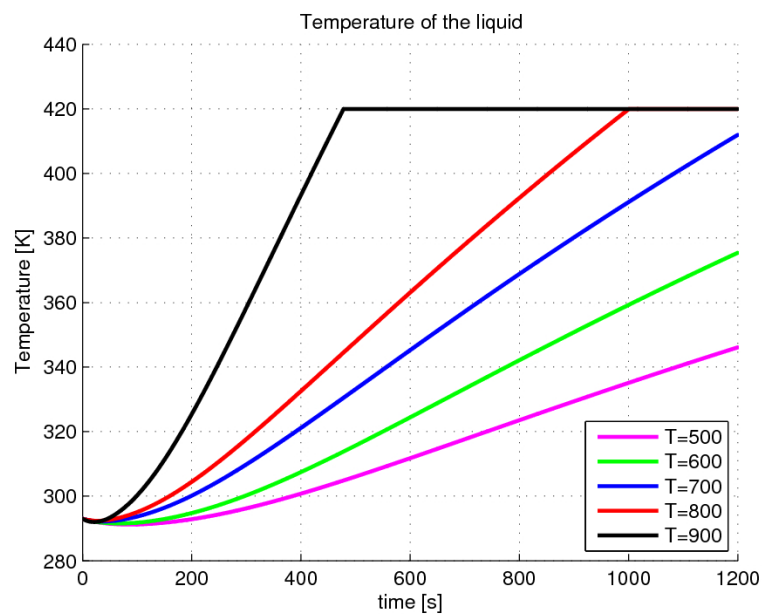


Figure 48:  $T_{gas}$  versus  $h$  fuel tank diffusive model

Figure 49:  $T_{gas}$  versus  $\dot{m}_{in}$  fuel tank diffusive modelFigure 50:  $T_{liq}$  versus  $T_{in}$  fuel tank diffusive model

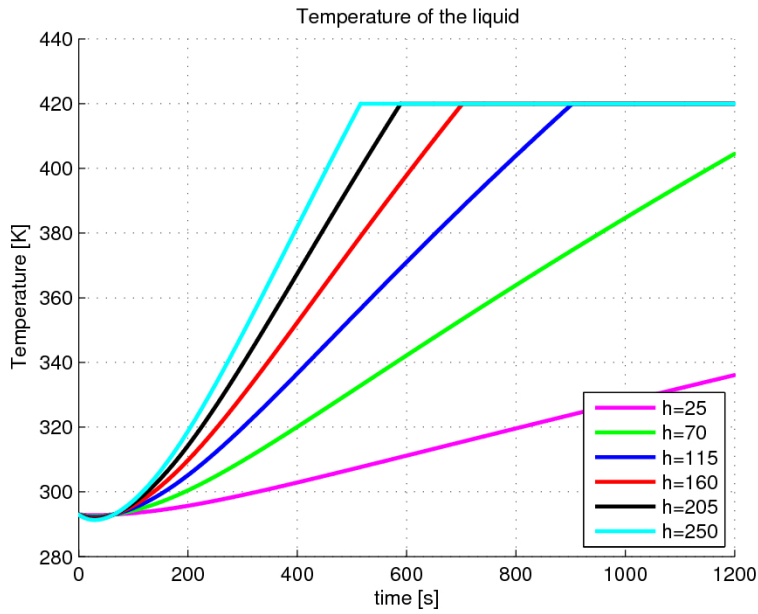


Figure 51:  $T_{liq}$  versus  $h$  fuel tank diffusive model

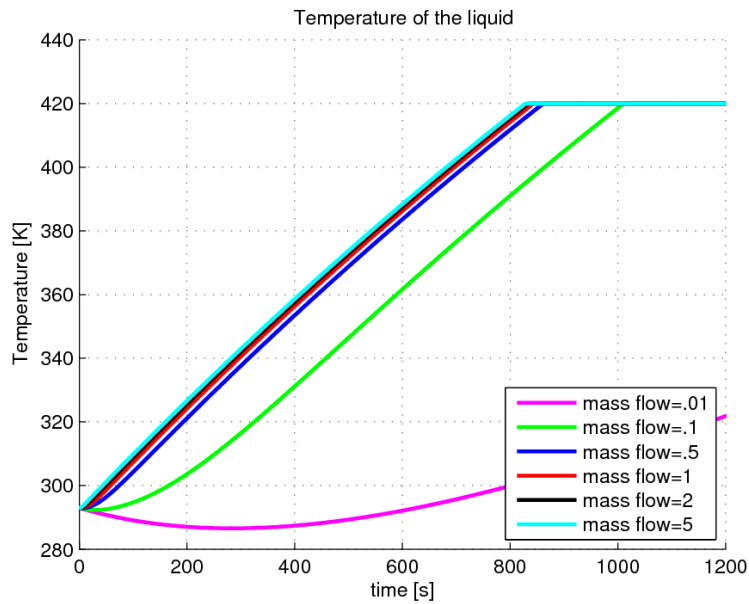


Figure 52:  $T_{liq}$  versus  $m_{in}$  fuel tank diffusive model

$\dot{m}_{in}$  of 0.01 kg/s, operating in this way the heat carrier given to LOX is controlled in order to prevent explosion.

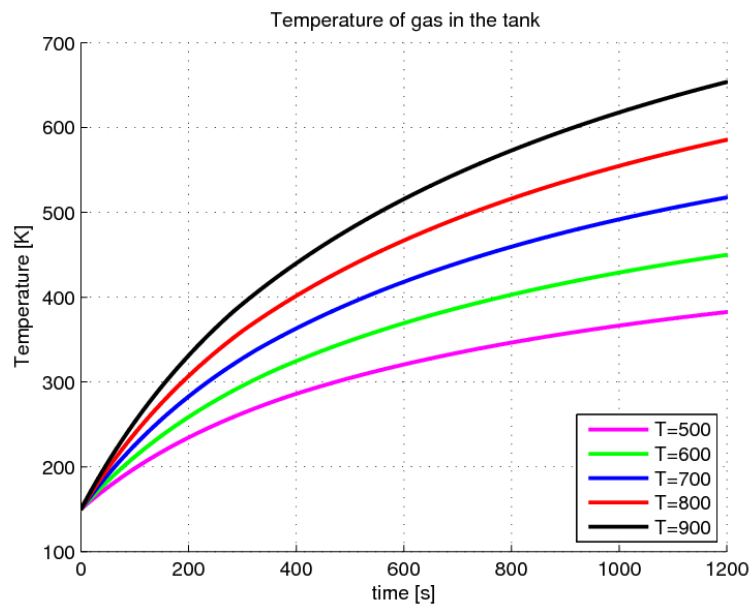


Figure 53:  $T_{gas}$  versus  $T_{in}$  oxidizer tank

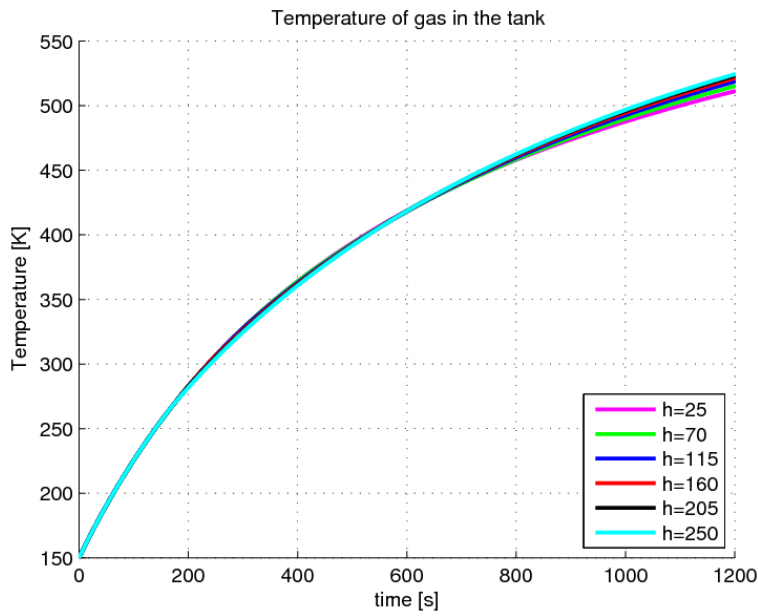


Figure 54:  $T_{gas}$  versus  $h$  oxidizer tank

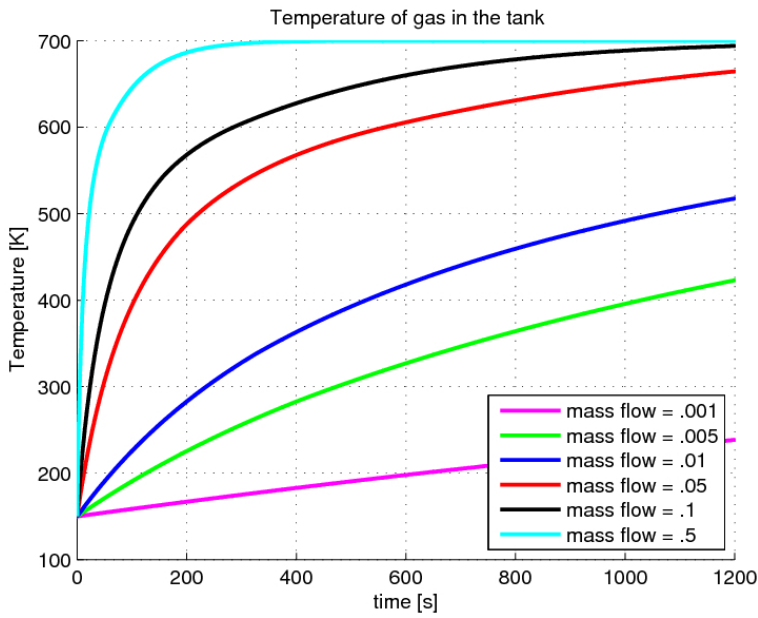
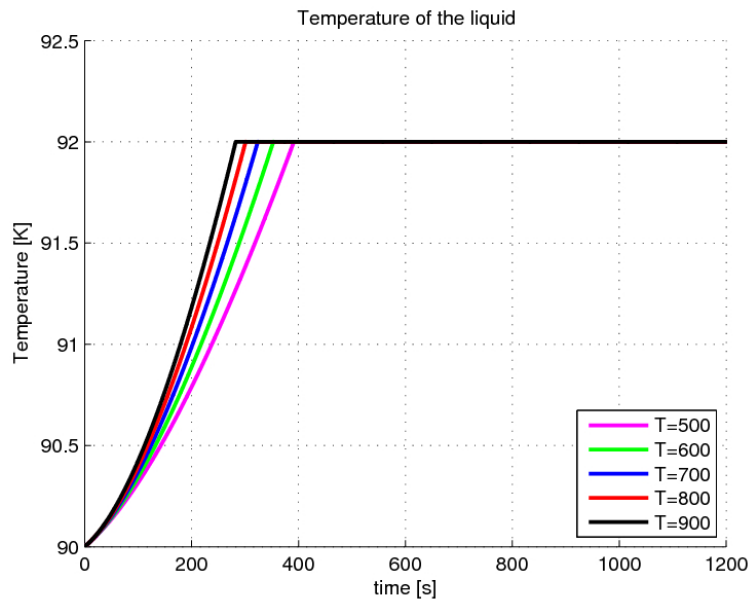
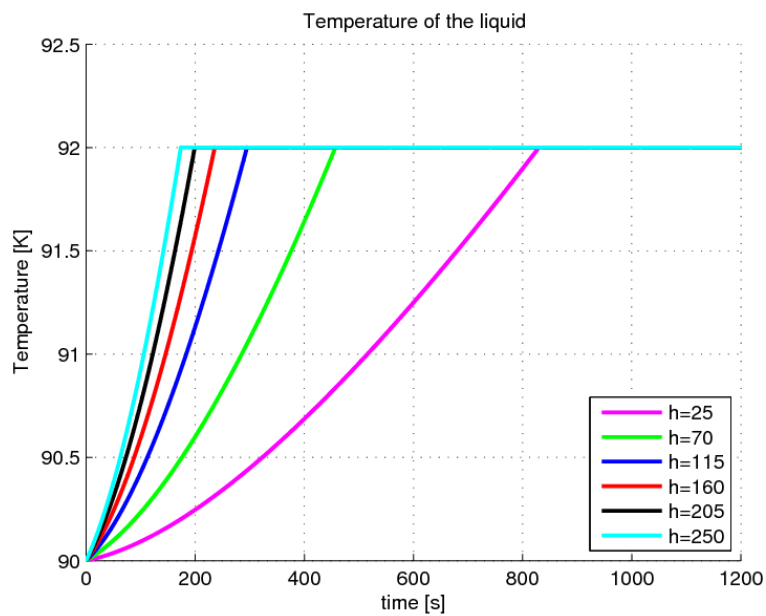


Figure 55:  $T_{gas}$  versus  $\dot{m}_{in}$  oxidizer tank



Figure 56:  $T_{liq}$  versus  $T_{in}$  oxidizer tankFigure 57:  $T_{liq}$  versus  $h$  oxidizer tank

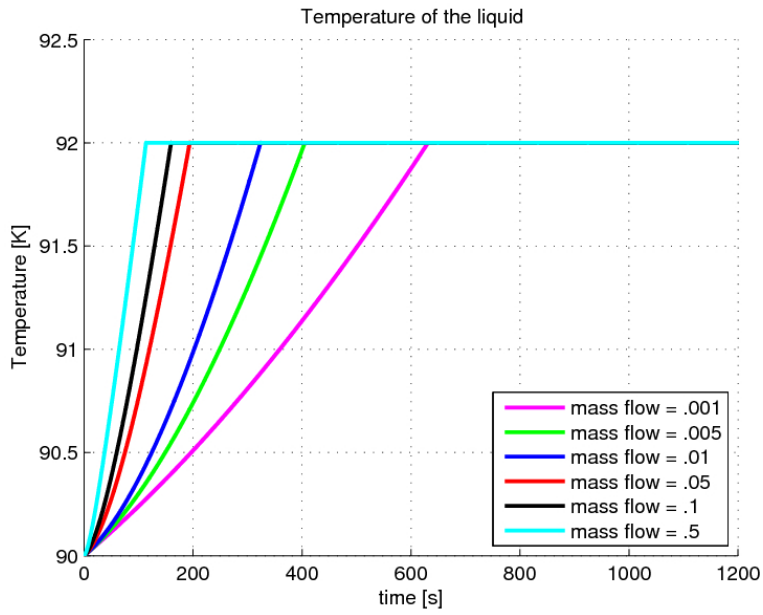


Figure 58:  $T_{liq}$  versus  $\dot{m}_{in}$  oxidizer tank

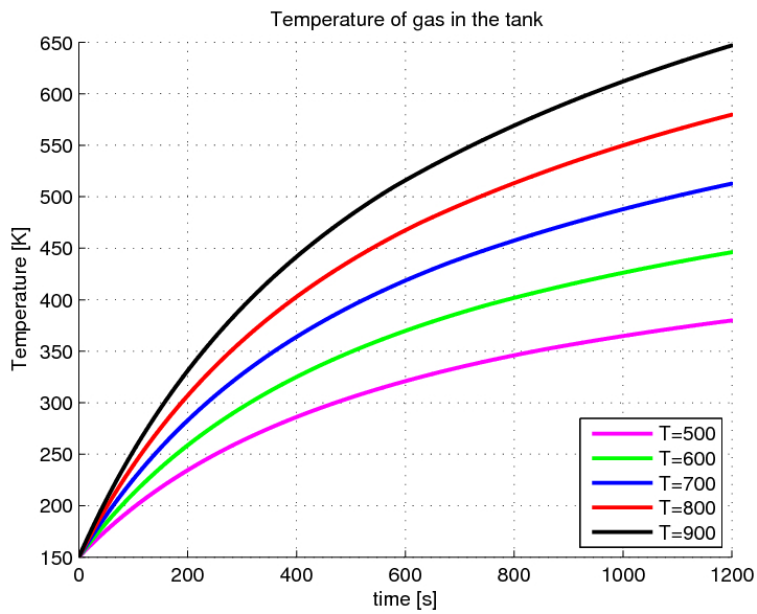
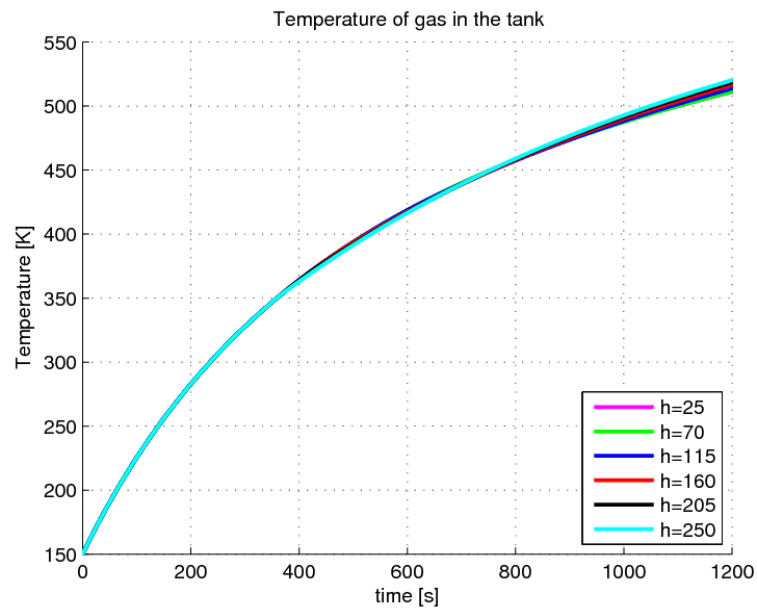
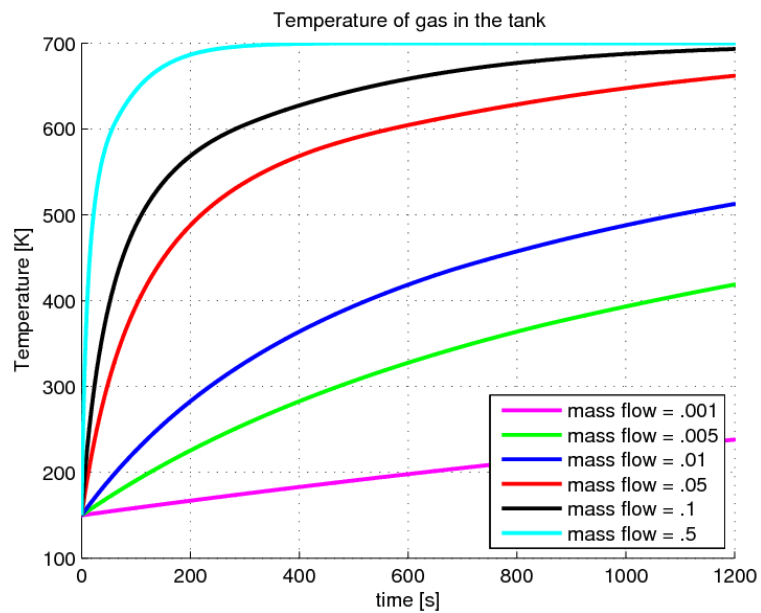


Figure 59:  $T_{gas}$  versus  $T_{in}$  oxidizer tank diffusive model

Figure 60:  $T_{gas}$  versus  $h$  oxidizer tank diffusive modelFigure 61:  $T_{gas}$  versus  $\dot{m}_{in}$  oxidizer tank diffusive model

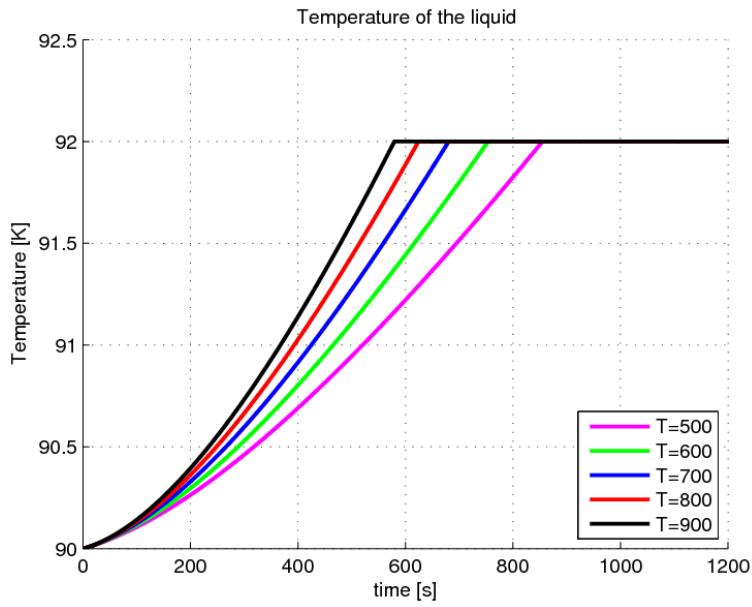


Figure 62:  $T_{liq}$  versus  $T_{in}$  oxidizer tank diffusive model

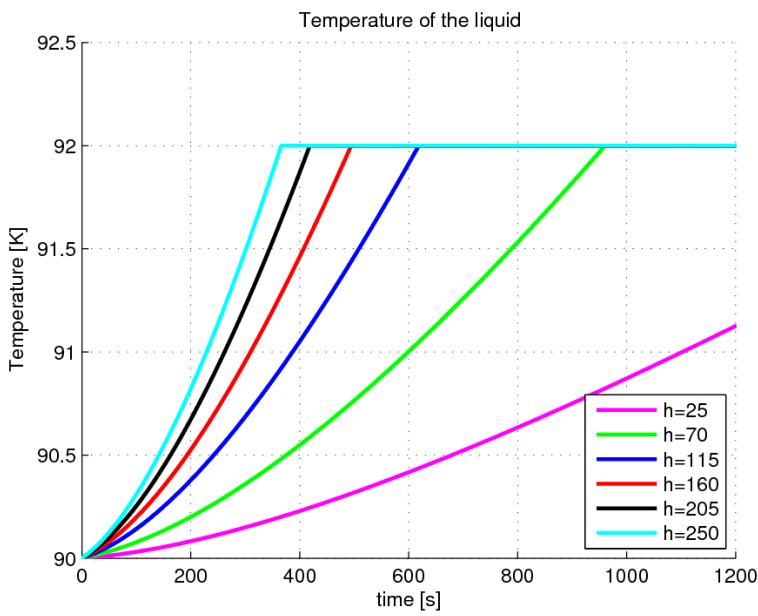


Figure 63:  $T_{liq}$  versus  $h$  oxidizer tank diffusive model

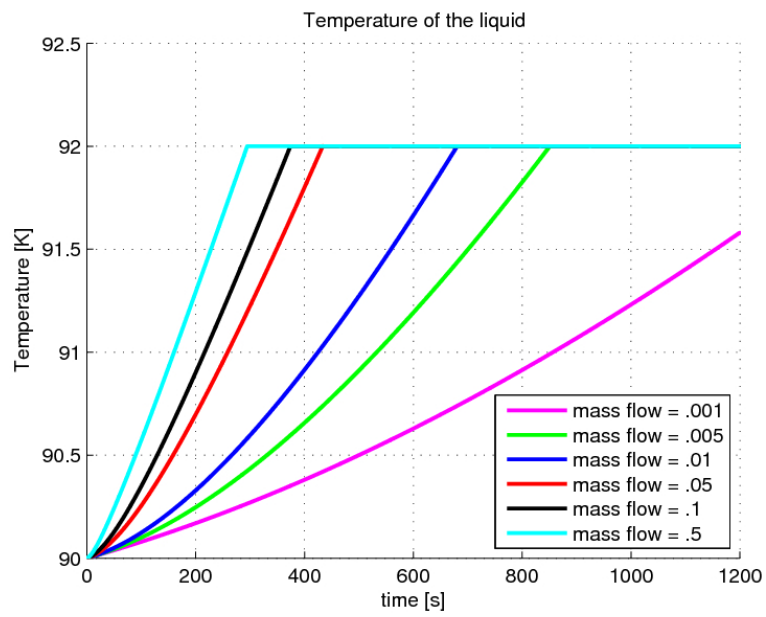


Figure 64:  $T_{liq}$  versus  $\dot{m}_{in}$  oxidizer tank diffusive model



## PRELIMINARY DESIGN OF THE SYSTEM

---

### 6.1 SYSTEM DESIGN

In this chapter is reported the general features of the system, which consist in:

- fuel tank
- oxidizer tank
- check valves
- pressure valves
- combustion chamber for gas generator for fuel tank
- combustion chamber for gas generator for oxidizer tank
- fuel and oxidizer injectors
- pipelines

Seen that the system should be equipped with:

- 117.58 kg of LOX ( $0.10305\text{m}^3$ )
- 44.37 kg or RP-1 ( $0.05220\text{m}^3$ )

it is necessary to develop a feed system that could inject the propellant into the gas generator chambers at a pressure of 8 bar. For the pressurization a system of Helium pressurized is the most suitable because the low weight of the system and the presence of LOX, that avoid the utilization of  $\text{N}_2$  as pressurization gas.

From the calculation to dimension the pressurization system we obtain the following feature for this component:

- Pressure of tank: 10bar
- Pressure of pressurization tank: 25bar
- Volume of pressurization tank:  $0.0785\text{m}^3$
- Mass of Helium: 0.17kg
- Material of tank: Titanium

- Mass of tank: 4.61kg

Making up budget propellant tank of Aluminum, which properties are reported in table 28

Density	2700[kg/m <sup>3</sup> ]
$\sigma_{sn}$	300[MPa]

Table 28: Aluminum properties

it is possible to evaluate the mass of these components.

- fuel tank mass:5.75kg
- oxidizer tank mass:9.02kg

Respecting the equation of continuity 6.1 and the considering the suggest condition of  $0.2 \leq M_c \leq 0.4$  the design of the combustions chambers has brought the following results:

$$\dot{m} = \rho \cdot u \cdot A_{cc} \quad (6.1)$$

- RP-1 gas generator combustion chamber diameter: 45 mm
- LOX gas generator combustion chamber diameter: 25 mm

To dimension the length of the chamber it has been taken in consideration a typical suggestion:  $2.5 \leq \frac{L_c}{d_c} \leq 3.5$ , even if it is necessary also consider the necessity of dilution, so the for this aim it is better to consider larger value to determine the length of the chamber.

- RP-1 gas generator combustion chamber length: 160 mm
- LOX gas generator combustion chamber diameter: 90 mm

To obtain the characteristics of the nozzle we report the result generated by CEA for the mixture coming out from tanks.

Choosing a  $A_e/A_t$  ratio of 20,  $C_F$  is known, so it is possible to calculate the  $A_t$  throat area. The thrust,  $T$  [18], is:

$$T = I_{sp} \cdot \dot{m} \cdot g_0 = P_c C_F A_t \quad (6.2)$$

From equation 6.2 we get  $A_t$  and from this value we can estimate all the parameter for the conic nozzle.

For the choice of the injector we must consider the situation presented in fig. ?? and ?? [19].

Figures ?? and ?? show several kind of injectors. For this system self-impinging stream pattern and doublet impinging stream pattern seem to be well suitable.



	Chamber	Throat	Exit	Exit	Exit	Exit	Exit
P [Bar]	4.0000	2.1749	0.09642	0.03409	0.01872	0.01227	0.00445
T [K]	3299.79	2859.35	1319.33	999.41	847.46	752.84	563.39
$\rho$ [kg/m <sup>3</sup> ]	1.678e-1	1.053e-1	1.011e-2	4.722e-3	3.058e-3	2.255e-3	1.092e-3
$M_m$ [kg/mol]	11.510	11.510	11.510	11.510	11.510	11.510	11.510
$\gamma$	1.3045	1.3104	1.3547	1.3742	1.3851	1.3923	1.4072
c [m/s]	1763.4	1645.2	1136.3	996.0	920.8	870.2	756.8
Mach	0.000	1.000	3.014	3.683	4.100	4.413	5.237

Table 29: Nozzle conditions

	Trhoat	Exit	Exit	Exit	Exit	Exit
$A_e/A_t$	1.0000	5.0000	10.000	15.000	20.000	40.000
$C^*$ [m/s]	2309.0	2309.0	2309.0	2309.0	2309.0	2309.0
$C_F$	0.7125	1.4831	1.5889	1.6353	1.6631	1.7163
$I_{vac}$ [m/s]	2900.7	3702.8	3865.5	3938.0	3981.6	4065.5
$I_{sp}^{sh}$ [m/s]	1645.2	3424.5	3668.7	3775.9	3840.0	3962.8

Table 30: Performance parameters

T	17,120 N
$A_e$	0.56m <sup>2</sup>
$A_t$	0.028m <sup>2</sup>
$A_c$	0.098m <sup>2</sup>
$\alpha_{conv}$	45°
$\alpha_{div}$	15°

Table 31: Nozzle features

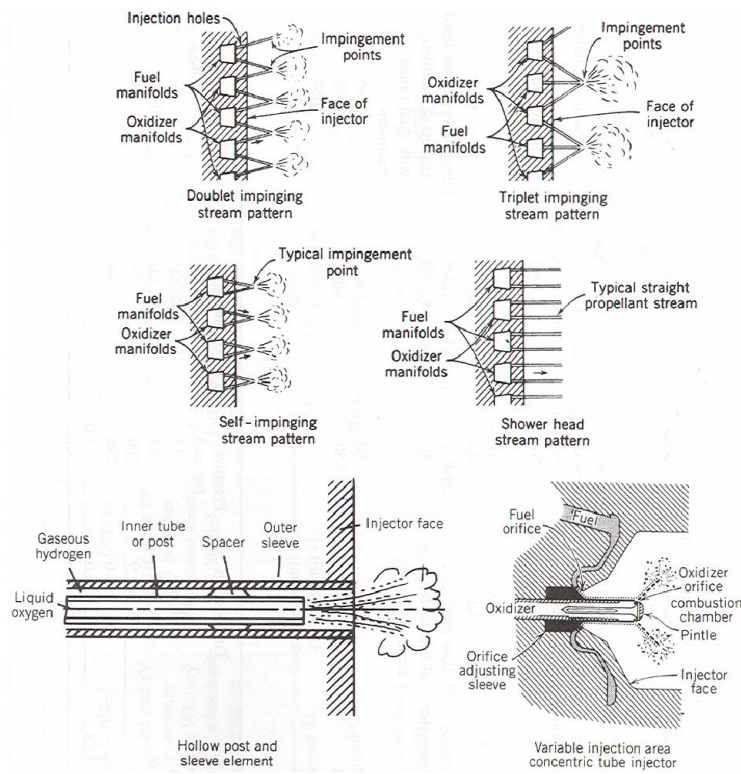


Figure 65: presentation of different kind of injector

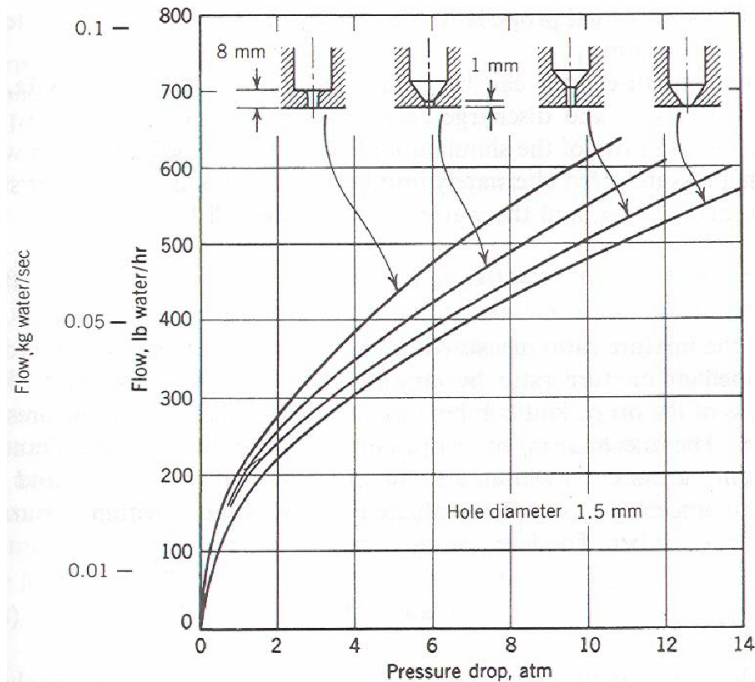


Figure 66: Performances of injector

## CONCLUSIONS

---

Through the simulation of the evaporation process it has been possible to develop a preliminary system that is able to gasify the residual propellant. With the adding of around 160 kg of propellant budget, in about 15 minutes for fuel tank and 13 minutes for oxidizer tank the system complete the evaporation of unused propellant. The system weights less than 25% of total unused mass and could be a useful solution for the problem of space debris.

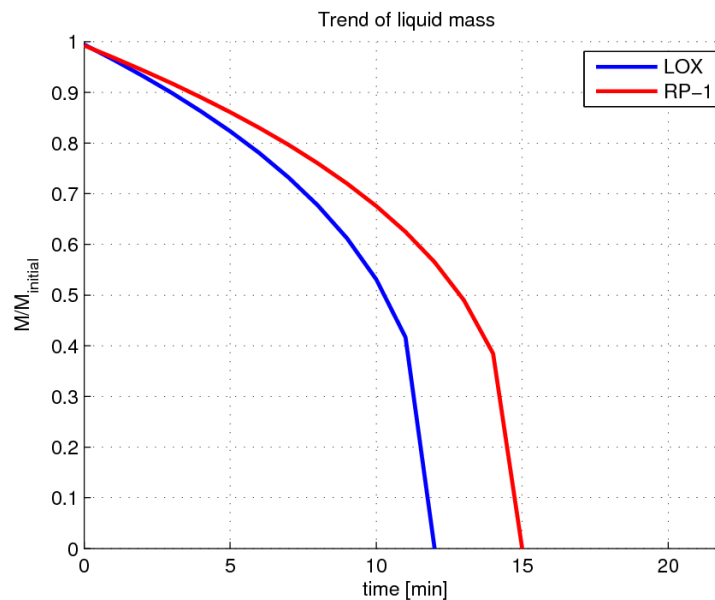


Figure 67:  $M_{liq}$  trend for LOX and RP-1

Figures 68 and 69 show that diffusion model seems to give a faster evaporation than the model based on convection.

### 7.1 FUTURE DEVELOPMENT

For future steps could be listed a lot of improvement to better the system. First of all it will be possible to make experiment in order to obtain a proper correlation for heat transfer between liquid and gas. Another point important to be focused is the determination of the correct attitude condition of the system in order to use the most suited correlation for natural convection, evaluating if it is necessary to use an approach with

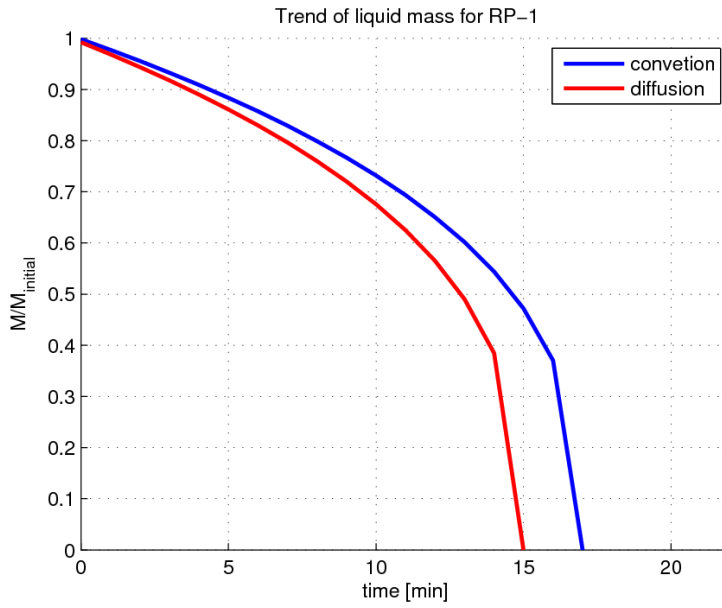


Figure 68: comparison of  $M_{liq}$  trend for RP-1

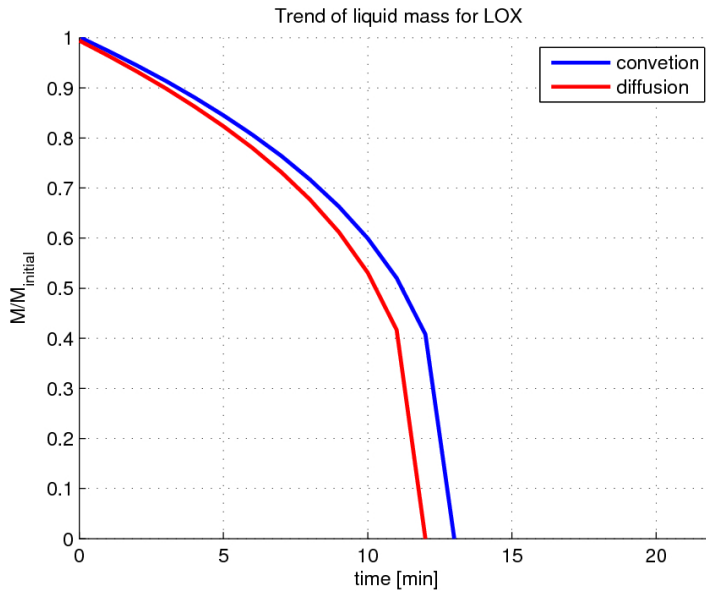


Figure 69: comparison of  $M_{liq}$  trend for LOX

absence of gravity to estimate  $h_{liq}$  [20] [21] [22] [23], or if the used correlation brings to correct results.

A CFD model will be very interesting and useful to develop because it will help on the study by making parametric simulation considering also the presence of bubbles, the fluid motion without using limiting hypothesis as here done.

Another interesting point of study is the use of sodium azide  $\text{NaN}_3$ , that is a salt, used in airbag with other compound such as  $\text{Fe}_2\text{O}_3$ ,  $\text{SiO}_2$  and so on, to produce warm gases, completely inert, because they mainly consist in  $\text{N}_2$ , by heating with an electric resistance [24] [25] [26]. By heating sodium azide it starts decomposing by its own one reached the temperature of 380K, and the warm gases produced have temperature around 500 - 600 K [27]. This solution maybe will not very suitable for the evaporation of RP-1 due to the low temperature of gases, but could be useful for LOX.



## BIBLIOGRAPHY

---

- [1] R. Reid, J. Prausnitz, and B. Poling. *The properties of gases and and liquids*. MacGraw-Hill Book Company, 4th edition, 1985.
- [2] B. Steigemeier, L. Meyer, and R. Taghavi. A thermal stability and heat transfer investigation of five hydrocarbon fuels: Jp-7, jp-8, jp-8+100, jp-10, and rp-1. *38th AIAA/ASME/SAE/ASEE Joint Propulsion Conference and Exhibit*, July 2002.
- [3] Incroprera, Dewitt, Bergman, and Lavine. *Fundamentals of heat and mass transfer*. Wiley, 6th edition, 2005.
- [4] Various authors. *Soyuz User's guide*, revision 0 edition, 2006.
- [5] T. Senechal. *Orbital Debris: Drafting, Negotiating, Implementing a Convention*. PhD thesis, Massachusetts Institute of Technology, june 2007.
- [6] S.V. Chekalin, V.I. Lukiyashenko, A.N. Kuznetsov, and V.P. Blagun. Study of causes and feasible measures to prevent further space environment pollution. *Proceeding of the second european conference on space - ESOC*, May 1997.
- [7] D. Wright. Space debris. *Physic Today*, October 2007.
- [8] V. Davidov, S. Kulik, M. Mikhailov, S. Chekalin, M. Yakovlev, and Y. Bulinin. Measures undertaken by the russian federation for mitigating artificial space debris pollution. *Proceeding of the fourth european conference on space debris - ESOC*, August 2005.
- [9] C. Bonnal. Design and operational practices for the passivation of spacecraft and launchers at the end of life. June 2007.
- [10] G. Sutton and O. Bilarz. *Rocket Propulsion Elements*. Jhon Wiley and Sons inc., 2001.
- [11] V. Trushlyakov. A mathematical model of the thermodynamic process of gasification liquid rocket fuel component. 2004.
- [12] Z.J. Wang, M. Chen, and Z.Y Guo. Nonequilibrium molecular dynamics simulation of evaporation and condensation. *International Conference "Passive and Low Energy Cooling 543 for the Built Environment"*, May 2005.
- [13] P. Rahimi and C. Ward. Kinetics of evaporation: Statistical rate theory approach. *Int. J. of Thermodynamics*, Mar. 2005.

- [14] J. O'Connell, J. Prausnitz, and B. Poling. *The properties of gases and liquids*. MacGraw-Hill Higher Education, 5th edition, 2007.
- [15] K. Pitzer. 77:3427. *J. Am. Chem. Soc.*, 1955.
- [16] H. Hanley, R. McCarty, and J. Sengers. Viscosity and thermal conductivity coefficients of gaseous and liquid oxygen. *NASA CR-2440*, 1974.
- [17] I. Witchterle. Natural convection to isothermal flat plate with a spatially nonuniform acceleration. *Ing. Eng. Chem.*, 1963.
- [18] R. Humble, G. Henry, and W. Larson. *Space propulsion analysis and design*. Macgraw-hill, 1995.
- [19] L. DeLuca. *Problemi energetici in propulsione aerospaziale*. Politecnico di Milano, 1998.
- [20] V. Pukhnchov. Mathematical model of natural convection under low gravity. 1991.
- [21] V. Polezhaev. Free convection in the internal problem: results and prospects. *Journal of Engineering physics and thermophysics*, 1996.
- [22] O. Goncharova. Microconvection in weak force fields. a numerical comparison of two models. *Journal of applied mechanics and technical physics*, 1997.
- [23] Y. Ma and J. Chung. An experimental study of critical heat flux in microgravity forced-convection boiling. *International Journal of multiphase flow*, April 2001.
- [24] Ignition enhancer coating composition for azide propellant. *U.S. Patent*, jan. 1981.
- [25] Breazeale. Gas generating composition. *U.S. Patent*, Jan. 1976.
- [26] Sidebottom. Gas generating compositions. *U.S. Patent*, May 1975.
- [27] Hamilton. Gas generating material. *U.S. Patent*, Spet. 1987.